THESIS

A MODELING APPROACH TO ESTIMATING SNOW COVER DEPLETION AND SOIL MOISTURE RECHARGE IN A SEMI-ARID CLIMATE AT TWO NASA CLPX SITES

Submitted by

Julie D. Holcombe

Department of Forest, Rangeland and Watershed Stewardship

In partial fullfillment of the requirements

for the Degree of Master of Science

Colorado State University

Fort Collins, Colorado

Summer 2004

COLORADO STATE UNIVERSITY

April 23, 2003

WE HEREBY RECOMMEND THAT THE THESIS PREPARED UNDER OUR SUPERVISION BY JULIE D. HOLCOMBE ENTITLED A MODELING APPROACH TO ESTIMATING SNOW COVER DEPLETION AND SOIL MOISTURE RECHARGE IN A SEMI-ARID CLIMATE AT TWO NASA CLPX SITES BE ACCEPTED AS FULFILLING IN PART REQUIREMENTS FOR THE DEGREE OF MASTER OF SCIENCE

Committee on Graduate Work

_____

_____

_____
Co-Adviser

_____
Adviser

_____
Department Head

ABSTRACT

A MODELING APPROACH TO ESTIMATING SNOW COVER DEPLETION AND SOIL MOISTURE RECHARGE IN A SEMI-ARID CLIMATE AT TWO NASA CLPX SITES

Snow cover depletion and soil moisture recharge are small segments, but crucial hydrological components for cryospheric regions of the earth. The abilities of a one-dimensional mass and energy balance model (SNTHERM) to predict snow cover depletion and Fast All season Soil STrength (FASST) to model the evolution of soil moisture recharge based on observed data from two NASA Cold Land Processes Experiment (CLPX) sites were evaluated. The objective was to investigate both model accuracies in predicting the observed parameters at Buffalo Pass near Steamboat and Illinois River located in North Park, both of which are located in the Colorado Rocky Mountains and are known for their differences in terrain and weather conditions.

The results from SNTHERM and FASST and the model performance statistics illustrate that the models overall fit to the observations were excellent at both locations. SNTHERM predicted the snow cover depletion date two days later than the observations at Buffalo Pass and only one day prior to the observations at Illinois River. The timing of snow accumulation and melt at Illinois River was in agreement with the observations at Illinois River, but the magnitude of snow depth was incorrect. The shallow and patchy nature of snow cover and the inconsistent meteorological parameters were problematic for SNTHERM. FASST correctly predicted the magnitude of seasonal soil moisture

storage at both sites, but soil moisture recharge prediction was challenging for the model. A lateral flow module and thorough soil data are thought to improve FASST's capability to predict the timing of soil moisture change. SNTHERM and FASST prove to possess the ability to predict snow cover depletion and seasonal soil moisture storage at two radically different field sites.

Julie D. Holcombe
Department of Forest, Rangeland and Watershed Stewardship
Colorado State University
Ft. Collins, CO 80521
Summer 2004

Acknowledgements

I would like to start off expressing my gratitude for the opportunity to complete my Master's degree by profusely thanking my dad. I feel very lucky to have such a friendship that forces me to see all the positive aspects of myself and has taught me to believe in myself when times were tough. My dad has not always agreed with my decisions, but has supported them and consequently, I have made him proud. I would not have completed this degree if my dad was not the wonderful person that he is. Although my mom was sick and not always supportive, I owe her thanks for the efforts that she made and the love that she gave. She would be proud of me for this accomplishment.

I have been extremely lucky and thankful for the chance to work with Kelly Elder. Even though I did not have the opportunity to take classes with Kelly, I was able to participate in field work and events, where I have obtained priceless knowledge about snow hydrology. Kelly is not only an excellent source of information, but is also a great person. Without Kelly's support and belief in my strengths, I would not have had this once in a lifetime opportunity to follow out a dream and gain the skills that I have gained.

I am also very appreciative to my committee: Steven Fassnacht, Susan Frankenstein and Greg Butters. Each one of them not only contributed to my thesis, but inspired me in such a way that I could not imagine them out of my committee.

I would also like to thank Bert Davis and CRREL for financial assistance throughout this project. I did not expect financial help, but was pleasantly surprised and very grateful.

The NASA CLPX team field members helped collect data for this project and Gus Goodbody assisted with much of the data management. I owe a huge thanks to everyone

involved. I would also like to thank Don Cline for allowing me to use the data collected as well as participate in the NASA CLPX.

Lastly, I would like to mention Jeff Deems, Debbie Zarnt, Tracy Phelps, Krista Northcott who have all assisted in proofreading, provided moral support and joined me in a few fun days off of work.

TABLE OF CONTENTS

LIST OF FIGURES

Chapter 6

LIST OF TABLES

CHAPTER 1. INTRODUCTION AND BACKGROUND

1.1. INTRODUCTION

Water stored in snowpacks and soils in the western United States is particularly important for natural ecosystems, public consumption and industry. Snowmelt accounts for approximately 80% of the soil moisture in semi-arid environments in the western United States (Marks and Winstral, 2002). The intricate process of snow cover depletion and soil moisture recharge is spatially and physically complex but an assessment of its behavior is essential for water balance approximations, climate-feedback research, remote sensing applications and hydrological modeling and forecasting (Hinzman and Kane, 1991; Shook et al., 1993; Baral and Gupta, 1997; Harms and Chanasyk, 1998; Liston, 1999; Cline et al., 2003).

The depletion of the snowpack and subsequent soil moisture recharge are dependent upon meteorological conditions, snowpack and soil properties, soil heat flux, antecedent soil conditions, vegetation and underlying topography (Willis et al., 1960; Granger et al., 1977; Male and Gray et al., 1981; Flerchinger and Saxton, 1987; Harms and Chanasyk, 1998; Faria and Pomeroy, 2000; Asch et al., 2001; Julander and Cleary, 2001). This paper shows that uncertainty in snow cover depletion and soil moisture recharge forecasting can be improved by models that are validated with high quality datasets (Cline et al., 2003).

1.2. BACKGROUND

Snow cover depletion is vital for modeling applications because its variability affects the energy balance, snow water equivalent (SWE), soil moisture recharge and thus the snowmelt runoff hydrograph (Male and Gray, 1981; Pomeroy et al., 1998). For example, as the snowpack ablates, the residual patchy mosaic of snow cover and vegetation governs the magnitude of energy emitted into the atmosphere and affects the temporal melting of the remaining snow cover (Liston, 1999).

The snow cover depletion depends on meteorological parameters as well as the physical and thermal properties of the snowpack (Male and Gray, 1981). Ablation is non-uniform due to land characteristics such as vegetation cover and topography (Marks and Winstral, 2001). Snow cover depletion can be estimated while accounting for vegetation cover and topography using areal-snow cover depletion curves (Baral and Gupta, 1997). These curves yield geographic location estimations of snow cover depletion.

Soil moisture recharge occurs when precipitation or snowmelt infiltrates into the soil matrix (Dunne and Leopold, 1978). Antecedent soil moisture and temperature play a major role in the infiltration of snowmelt and run-off (Willis et al., 1960; Harms and Chanasyk, 1998). Typically, snowmelt run-off occurs if the soils are saturated or contain a frozen layer prior to the onset of snowmelt (Gray et al., 2001; Julander and Cleary, 2001). Conversely, dry soils prior to snowmelt can absorb and retain the meltwater from the snowpack, which can reduce streamflow (Julander and Cleary, 2001).

The evolution of soil moisture storage within soils is complex and depends on soil type, meteorological conditions, evapotranspiration, snowpack characteristics and

topography (Dunne and Leopold, 1978; Male and Gray, 1981). These parameters also affect the soil drainage, all of which causes soil moisture to be highly spatially and temporally variable (Dunne and Leopold, 1978; Asch et al., 2001).

1.2.1 Snow Cover Depletion and Soil Moisture Recharge Studies

Willis et al. (1960) studied the effects of fall soil moisture and presence of snow on the depth of freezing in the soil matrix and spring run-off. Field plots were designed with dry, medium and wet moisture levels. Each moisture level plot had a control plot, which consisted of the natural snowpack and treatments of snow added to the natural snowpack, and a snow-free treatment. The dry soil froze deeper and faster than the wet soil. The plots without snow cover lost soil moisture. Runoff occurred in the plots with the natural snowpack and the plots with higher moisture levels. They concluded that fall soil moisture levels combined with winter weather conditions regulated the depth of freezing in the soil matrix and spring run-off.

Harms and Chanasyk (1998) investigated the variability in snowmelt runoff and soil moisture recharge in relation to differences in aspect, slope, and pre-winter soil moisture. The fall soil moisture could not be used in this analysis because of premature melting during the winter. There was no correlation found between the quantity of runoff at similar slopes and aspects even though aspect had a major influence on timing and quantity of runoff.

Julander and Cleary (2001) discussed the importance of soil moisture to improve forecasts of streamflow from snowmelt. They concluded that a total water balance would

be necessary to quantify the contributions of soil moisture to streamflow, but that soil moisture did have an impact on streamflow.

1.2.2 Model Applications

The physical processes of snow cover depletion and soil moisture recharges are fairly well understood (Harms and Chanasyk, 1998; Julander and Cleary, 2001). Predictions of the hydrological elements at a point in space need more attention. Model applications that physically represent hydrologic data are tools that assist in site-specific hydrologic predictions. Models that misrepresent hydrologic data are useful because they force scientists to narrow down the problem. The following research presented focused on snowmelt and water balance approximations for predictions of soil moisture, but not snow cover depletion and soil moisture recharge.

Rowe et al. (1995) used observational snowmelt data from a Greenland ice sheet and compared the data to the predictions made by a one-dimensional mass and energy balance model (SNTHERM). The ice sheet was treated as the underlying substrate of the snowpack instead of a soil layer. Parameter adjustment was performed in an attempt to accurately represent the physical conditions of the snowpack. For example, the user entered the daily-calculated albedo instead of using a default albedo value within the model. The density was overestimated at the bottom 0.05m of the snowpack presumably because the meltwater refroze at the snowpack-ice boundary. Instead, an actual slush layer developed at the base of the snowpack, which was not represented by SNTHERM since it was designed to drain the water into the underlying substrate. Overall, SNTHERM was found to agree well with the observations.

Gustafsson et al. (2001) compared SNTHERM to a single layer snow model, Soil-Vegetation-Atmosphere Transfer (SVAT) in a study of the surface energy balance of a snowpack in central Sweden. Their objective was to evaluate two one-dimensional models for their heat and mass flux predictions between the atmosphere-snow-soil boundaries depending on snowpack surface heat exchange. The SVAT model treated the snowpack as a homogeneous layer and an adaptation of SNTHERM was used as the multi-layered model. In general, the models predicted the snow accumulation and melt within one standard deviation from the mean of each variable, respectively. However, there were discrepancies in the energy parameters such as daytime net radiation. Some of the discrepancies were attributed to user inputs of parameters and measurement interpolation techniques. The models were shown to be in reasonable agreement despite the internal configuration differences.

Groffman et al. (1999) applied SNTHERM to a hardwood forest region to test whether or not the model could accurately predict soil temperatures and frost for a pilot study. The researchers compared a control plot with a natural snowpack to a study plot in which the ground was kept free of snow. The results showed that SNTHERM predicted the soil temperatures accurately in both plots, which suggests that SNTHERM accurately took into account the snow depth.

Hardy et al. (1998) tested the ability of SNTHERM, combined with a hybrid Geometrical Optical Radiative Transfer model (GORT), in predicting snow ablation in a boreal forest. The models relied on meteorological variables, soil temperatures, tree stand characteristics and snow data. An adjustment of the albedo was employed in SNTHERM under certain radiation conditions to test for more accurate predictions of

snow ablation. These methods were successful since both models agreed well with the observations.

Pomeroy et al. (1998) used the Canadian Land Surface Scheme (CLASS) and developed a new algorithm to predict snow cover depletion in a prairie environment. Estimations of snow cover depletion from the new algorithm and the CLASS model were compared. They found that the method that uses the new algorithm and CLASS considerably underpredicted the timing and rate of the snowmelt even though the model underestimated the net energy flux. They concluded that overestimation of ground heat when soils are frozen contributed to the model error and that more detailed information need be included in the model regarding snowpack energetics and soil heat movement.

Jin et al. (1999) used a simpler modification of SNTHERM to predict snow depth. This model did not estimate the vapor phase, vertical movement of water due to gravity and only three layers of the snowpack were employed in the predictions. To represent a single snow depth value within a grid square, three fractions of snow depth were parameterized. The model performed more accurately during the winter period than during the spring period. The snowfall was measured in a different location than the snow depth and only one snow depth measurement in a point location was compared to the simulations that represented an areal measurement. These reasons were thought to be the cause of differing modeling accuracies even though, overall, the model agreed with the observations.

Cherkauer et al. (2002) used a unique Soil-Vegetation-Atmosphere transfer scheme (SVATS) that incorporated a full energy balance, estimated soil moisture and represented baseflow in a cold region. This Variable Infiltration Capacity (VIC) model

also included a routine for calculating complete and patchy snow cover extent in a sub-grid area. The soil moisture was spatially estimated by using the variable infiltration curve. The researchers also included an algorithm that predicts the variable spatial-scale soil frost condition as opposed to the previous prediction that estimated a uniform frozen state of the soil. They concluded that the new algorithm allows snowmelt infiltration in the unfrozen zones of the soil, which results in a lower discharge and thus less flood predictions.

Levine and Knox (1997) applied a modified version of the Residue model that describes mass and energy flux through a soil-crop-residue-atmosphere system in forested site. The modified FroST (frozen soil temperatures) was used in conjunction with snow and vegetation properties to predict snow depth and soil temperature. Separate snow nodes were not added. Instead, the soil node was altered to include snow. They used SNTHERM to obtain representative snow properties such as snow grain size. SNTHERM generated the snow density and thermal conductivity values to be used in the FroST model. The FroST and SNTHERM model were coupled by using FEDMOD (Forest Ecosystem Dynamics Modeling Environment). They found that adding an organic composition to the soil system effected the insulation. The thermal and hydraulic properties were affected when modifications were made to soil thickness and water-holding capacity. The results of the modeled soil temperature and snow cover compared favorably with the observations. Soil temperature simulations could be improved with enhanced routines for transpiration, radiation and snowpack data.

There are currently no published studies to be included in this section regarding FASST. Frankenstein (2003) provides validation information for certain modules within FASST.

Physically based modeling approaches to estimating snow and soil characteristics are not new. Many papers have focused on SWE and not snow depth. Snow depth is important for estimations of SWE, potential runoff, and information regarding insulation of soil for biogeochemistry studies. Few studies have included point snow depth for purposes of snow cover depletion estimations and point soil moisture underlying soil moisture simulations. Neither SNTHERM nor FASST have been used to estimate snow cover depletion and soil moisture recharge.

CHAPTER 2. STUDY SITES

2.1. COLD LAND PROCESSES EXPERIMENT

The NASA Cold Land Processes Experiment (CLPX) was developed in order to: identify the role of the snowpack in the storage of water resources by quantifying many snowpack properties; improve the representation of snow in models by taking measurements on various distributed spatial and temporal scales; provide high-quality and abundant databases of snow and soil characteristics; and improve remotely sensed measurements of snow properties and soil moisture. The CLPX data collection period took place during the 2002 and 2003 snow seasons and included an observational and remote sensing dataset of snow and soil conditions. CLPX study sites were located in central Colorado: Fraser Experimental Forest, Rabbit Ears Pass and in North Park. Each of these study sites was chosen for their unique snowpack, meteorological and physiographic characteristics (Cline et al., 2003).

2.2. FIELD SITES

Three locations in Colorado, Fraser Experimental Forest, Rabbit Ears Pass, and North Park were used, with each location containing three Intensive Study Areas (ISA's). The ISA's are a one kilometer square grid with a meteorological station located near the center that records micrometeorological time series data, snow depth, soil moisture and soil temperature profiles. Study sites were chosen from the NASA CLPX field sites. Two sites were chosen from the nine CLPX meteorological stations in order to explore SNTHERM and FASST's predictive abilities at two radically different sites. The sites

chosen were Illinois River in North Park and Buffalo Pass near Steamboat Springs (Figure 2.1).

Rabbit Ears Pass has moderate relief, rolling hills and mixed vegetation of coniferous and deciduous forests. The snowpacks are moderate to deep. The vegetation type in this ISA is dominated by Englemann spruce (*Picea englemannii*) and alpine fir (*Abies lasiocarpa*). The soil type is a highly organic peat and the mean elevation is 3144m.

North Park is characterized by windy, low relief prairie terrain with a vegetation characteristic of grassland. The snow is generally shallow and windswept which allows the development of frozen soils. This ISA is approximately 93% cropland or pasture, and 6% shrub/brush rangeland with a mean elevation of 2480m and a soil type of inorganic sandy, silty, gravelly clay.

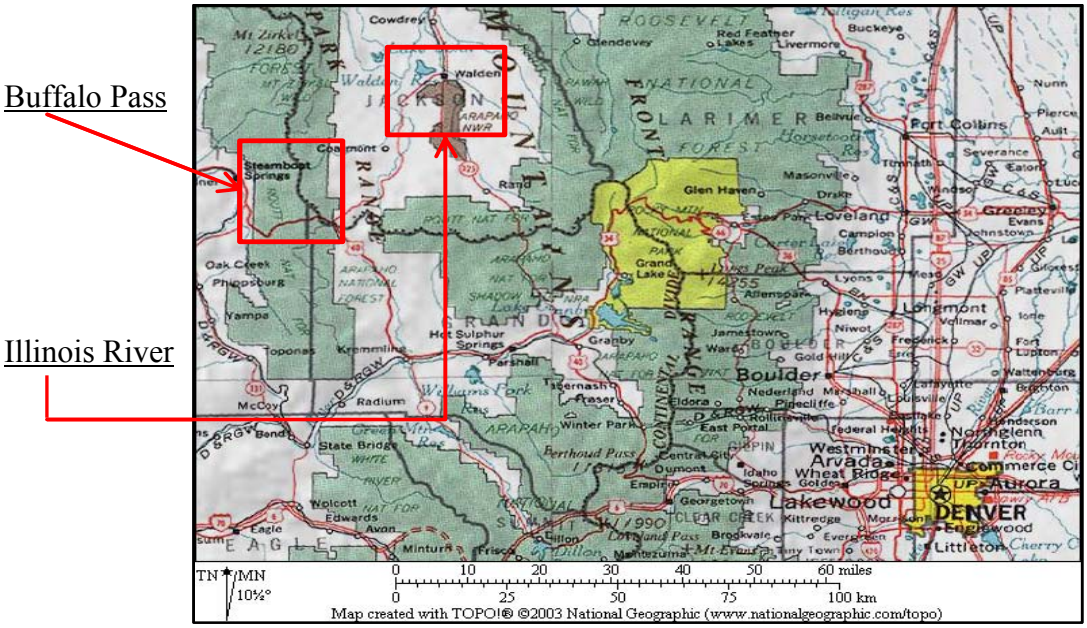

Figure 2.1. NASA CLPX Buffalo Pass and Illinois River field sites.

CHAPTER 3. MODELS

3.1. SNTHERM

SNTHERM is a one-dimesional model that was constructed primarily to predict surface temperatures of the snowpack. The model must be supplied with continuous meteorological parameters, and initial snowpack layer data. There is no limit to the number of input snowpack layers to initialize the model. See Figure 3.1 for a flow chart of SNTHERM.

SNTHERM uses meteorological input data and predicts outputs such as snow depth, snowpack temperature profiles, and snow water equivalent by using conservation of energy, momentum and mass equations such as Darcy's law for water flow, Fourier's law for conductivity of heat flow (i.e. energy) and interpolation methods. Additional empirical and numerical approximations are integrated into SNTHERM in order to predict the snowpacks changing physical properties with respect to meteorological variations. For example, specific enthalpy equations are used to estimate the thermodynamic energy of the snowpack while radiation entering the snowpack is estimated from an empirical fit.

For the purposes of this research, only the thermal and mass fluxes through the snowpack will be discussed. Therefore, the only internal configurations of SNTHERM discussed in this paper will be associated with the heat and water fluxes. See Appendix A for parameter definitions. Further inquiries about the design of SNTHERM should refer to the technical documentation for the model (Jordan, 1991).

The model predicts the thermal properties of the snowpack and fluid flow through the snow media by applying conservation equations in integral form. This method allows the heat and mass flux to be conserved over the volume of the snow and soil layers. The conservation approach to predicting fluxes permits the model to physically represent the heat movement through the snow strata instead of interpolating the flux. The snow and soil layers are defined in the model by a finite differencing grid. The integral form of the conservation equations is expressed as:

$$\partial/\partial t \int_v \gamma_b \Omega dV = avg(-\sum_b \int_s JdS) + \int_v avg(SdV) \quad (1)$$

time rate of change — fluxes — source term

where V is the volume of the snow or soil layer or control volume, Ω is the heat or amount of water being conserved, J is the flux, S is the source density. Equation (1)'s summation symbol in the flux term refers to summation over the constituents (b). The "avg" averages over time. The averages in equation (1) are calculated by the Crank-Nicolson method as:

$$avg\ \chi = 0.5[\chi^{t-\Delta t} + \chi^{t}] \quad (2)$$

where the $\chi^{t-\Delta t}$ and χ^{t} represent the past and present values of heat, mass of water, etc. respectively. t is usually between 5 and 900 seconds, but is adjusted internally to ensure numerical stability. γ_b is the bulk density of the snowpack, where b is i,l,v or a, which

stands for ice, liquid water, water vapor, or air components of the snowpack. The bulk density of the snowpack is defined as:

$$\gamma_b = \theta_b \rho_b \tag{3}$$

where θ_b is the volume fraction of the air, ice, liquid water, or water vapor, and ρ_b is the intrinsic density of the component. The intrinsic density is defined as the mass of b per unit volume of b. The conservation equations expressed in integral form are for a non-homogeneous quantity being conserved, bulk density, and source density within the snow or soil layer.

If the quantity being conserved, bulk density, and source density remain uniform throughout the snow or soil layer, the conservation equation reduces to:

$$\partial/\partial t \gamma_b \Omega \Delta z = - \Sigma avg[J^{j+1/2} - J^{j-1/2}] + S\Delta z \tag{4}$$

where z is the layer thickness of the snow or soil, j is the nodal index of the control volume, j+1/2 is the upper boundary of the layer j, and j-1/2 is the lower boundary of the layer j and J refers to convective flux, diffusive flux or a combination of the two mechanisms. The conductive - diffusive flux component is represented by:

$$avg[J^{j+1/2} - J^{j-1/2}] = -avg[(D\partial\Omega/\partial z)^{j+1/2} - (D\partial\Omega/\partial z)^{j-1/2}] \tag{5}$$

where D is the diffusion coefficient. The net convective flux component is represented by:

$$\text{avg}[J^{j+1/2} - J^{j}] = \text{avg}[(q\Omega)^{j+1} - (q\Omega)^{j}] \quad (6)$$

where q is the mass flux (Jordan 1991).

Figure 3.1. SNTHERM flow chart.

3.2. FASST

FASST is a one-dimensional model that was mainly designed to predict the condition of the ground for vehicle mobility purposes with the presence of a snowpack and without. The model requires a continuous input of meteorological data and initial soil layer data. See Figure 3.2. for a flow chart of FASST.

With respect to the internal configuration modules of FASST, only the modules relevant to this research, including, soil temperature, soil moisture, ground state, snow depletion, meltwater generation, and ice thickness will be discussed. Further inquiries regarding the design and numerical solutions of FASST should refer to the draft technical documentation (Frankenstein, 2003). The general output of the model includes meteorological parameters, surface conditions and soil profile information. See Appendix A for parameter definitions.

Soil temperature module

The thermal properties of the soil as predicted by FASST uses the heat flow equation:

$$\partial T/\partial t = \partial/\partial z\ (k\partial T/\partial z) - c_w/c_d*v\partial T/\partial z = \partial k/\partial z*\partial T/\partial z + k\partial^2 T/\partial z^2 - c_w/c_d*v\partial T/\partial dz + l_{fus}/c_{d*}\rho_i/\rho_w*\partial\theta_i/\partial_t \quad (7)$$

where T represents the temperature, z is depth, t is time, c_w is the specific heat of water, k is the thermal diffusivity and c_d is the soil specific heat, v is the rate of water motion, ρ_i is

the density of ice, ρ_w is the density of water and θ_i is the volumetric ice content. Boundary conditions that apply to the temperature are:

$$R_{\downarrow} - k\partial T/\partial z - 0.08 = 0 \; ; \; z = \text{bottom} \tag{8}$$

$$F(T) = (1-\alpha)S_w + R_{\downarrow} - R_{\uparrow} + H + L - P + \kappa\partial T/\partial z + l_{fus*}\rho_i/\rho_w + \partial\theta_i/\partial_t + \Delta z - vc_dT = 0; \quad z = 0 \text{ m} \tag{9}$$

where $R_{\downarrow}$ is incoming infrared radiation, $R_{\uparrow}$ is emitted infrared radiation, κ is the thermal conductivity of the surface, α is the albedo of the surface, S_w is the net solar radiation, H is the sensible heat, L is latent heat and P is heat from precipitation energy.

Soil moisture module

Darcy's Law, conservation of mass and the van Genuchten equation are integrated into FASST in order to predict the evolution and conductivity of moisture in the soil matrix. Darcy's law is as follows:

$$v = K\partial h/\partial z \tag{10}$$

where K is the hydraulic conductivity of the soil, h is the total head and ż is positive depth below the surface of the soil. In an unsaturated soil, the conservation of mass is:

$$\partial\theta_l/\partial t = -\partial v/\partial z - \rho_i/\rho_w * \partial\theta_i/\partial_t + \text{sources} - \text{losses} \tag{11}$$

where θ_l is the volumetric water content and t is time.

The boundary equations that apply to conservation of mass equations are:

$$q_{top} = -E + C + P + (h_{pond} + h_{,i\ melt} + h_{,s\ melt}) / \Delta t;\ z = 0\ m \quad (12)$$

$$q_{bot} = K \sin(slope)\ z = bottom \quad (13)$$

where q is mass flux, E is evaporation rate, C is the condensation rate, h_{pond} is the head due to ponding water at the soil surface, $h_{,i\ melt}$ is the head from melting ice, and $h_{,s\ melt}$ is the head due to melting snow.

The van Genuchten equation calculates the non-linear relationship between pressure head and volumetric soil moisture to determine the hydraulic parameters and is as follows:

$$\theta = \theta_R + (\theta_{max} - \theta r) / (1 + |\psi\alpha|^N)^{\ m} \quad (14)$$

where θ_R refers to residual water content, θ_{max} refers to the maximum water content, ψ is the pressure head, α refers to the reciprocal bubbling pressure head, N is a constant related to the pore size of the soil and

$$m = 1 - 1/N \quad (15)$$

Ground state module

This module estimates freezing or thawing with depth in the soil matrix by calculating the energy balance. The nodal energy is defined by:

$$\text{node energy} = \Delta Q_1 = |\, T_i - 273.15| \, \Sigma \theta_e \rho_e c_e \qquad (16)$$

where T_i is the nodal temperature, e represents dirt, water, ice or air, θ_e is the volumetric fraction of the constituents, ρ_e is the density of the constituent and c_e is specific heat. The energy in the soil matrix prior to the complete freezing or thawing of the soil is dealt with in FASST by:

$$\text{freeze energy} = Q_2 = l_{fus} \, (\theta_l - \theta_r) \, \Sigma \theta_e \rho_e c_e \qquad (17)$$

$$\text{thaw energy} = Q_2 = -l_{fus} \, \theta_i \, \Sigma \theta_e \rho_e c_e$$

where l_{fus} is the latent heat of fusion for water, θ_l is the actual volumetric fraction of water and θ_r is the minimum volumetric water content for the corresponding node. The evolution of θ_i is calculated by:

$$\Delta \theta_i = \rho_w / \rho_i \, * \, \min(Q_1 | Q_2|) / l_{fus} \qquad (18)$$

Snow accretion, depletion and meltwater outflow module

For this module, only the evolution of snow depth, depletion and meltwater generation of the snowpack will be discussed in this paper. The depth of the snowpack is calculated by the same method used in SNTHERM. The difference is that FASST uses the SNAP model, which only allows a single layer snowpack. The model estimates densification, and then snow depth is calculated from this estimation as:

$$|1/D_s * \partial D_s / \partial t|_{metamorphism} = -2.778 \text{x} 10^{-6} c_1 c_2 \exp\,[-0.04T] \qquad (19)$$

$$c_1 = 1, \ \rho_i \leq 0.12;$$

$$c_1 = \exp[-46(\rho_i - 0.15)], \ \rho_i \geq 0.12$$

$$c_2 = 1 + f_l$$

where D_s is the snow depth, t is time, T is temperature, ρ_i is the density of ice and f_l is the wet fraction of the snowpack. Next, the weight of the snowpack is taken into consideration by:

$$|1/D_s * \partial D_s/\partial t|_{overburden} = - avg(P_s)/\eta \quad (20)$$

where is $avg(P_s)$ is the average load pressure in the snowpack and η is the viscosity coefficient which is represented by:

$$\eta = \eta_o \exp(0.08T + 28\ \rho_t) \quad (21)$$

$$\eta_o = 5E{+}08$$

where ρ_t is the combined density of solid and liquid within the snowpack. To estimate the snowmelt, FASST uses a surface energy balance equation for each time step as:

$$I_{top} = I_{sw\downarrow}\ (1 - \alpha_{top}) + I_{ir\downarrow} - I_{ir\uparrow} + I_s + I_l + I_c \quad (22)$$

where I_{top} is the input of energy at the top of the snowpack, $I_{sw\downarrow}$ is the incoming solar radiation, α_{top} is the surface albedo, $I_{ir\downarrow}$ is the incoming longwave radiation component, $I_{ir\uparrow}$ is the outgoing longwave radiation, I_s is the sensible heat flux, I_l is the latent heat flux and I_c is the convective heat flux.

Ice thickness module

The growth of an ice layer is estimated by calculating the fraction of precipitation that goes through the freezing process by:

$$f = (\Sigma \text{ heat fluxes - latent heat flux})/\text{latent heat flux} \quad (23)$$

where the fluxes are the same as in equations (9), (10), and (11) under the soil thermal module. The ice thickness per unit area is represented by:

$$H_i = fP(\Delta t)\rho_w/\rho_i \quad (24)$$

where P is the precipitation rate, Δt is the time step, ρ_w and ρ_i is the density of water and ice respectively. The decomposition of the ice layer is calculated by:

$$h_i = q_{net}\,(\Delta t)/\rho_i\, l_{fus};\ \ T_s \geq 273.15 \quad (25)$$

$$h_i = q_{net}(\Delta t)/\rho i(l_{fus} - c_i T_s);\ \ T_s \leq 273.15$$

where q_{net} is the heat flux at the snow surface, l_{fus} is the latent heat of fusion, c_i is the specific heat of ice and T_s is the surface temperature.

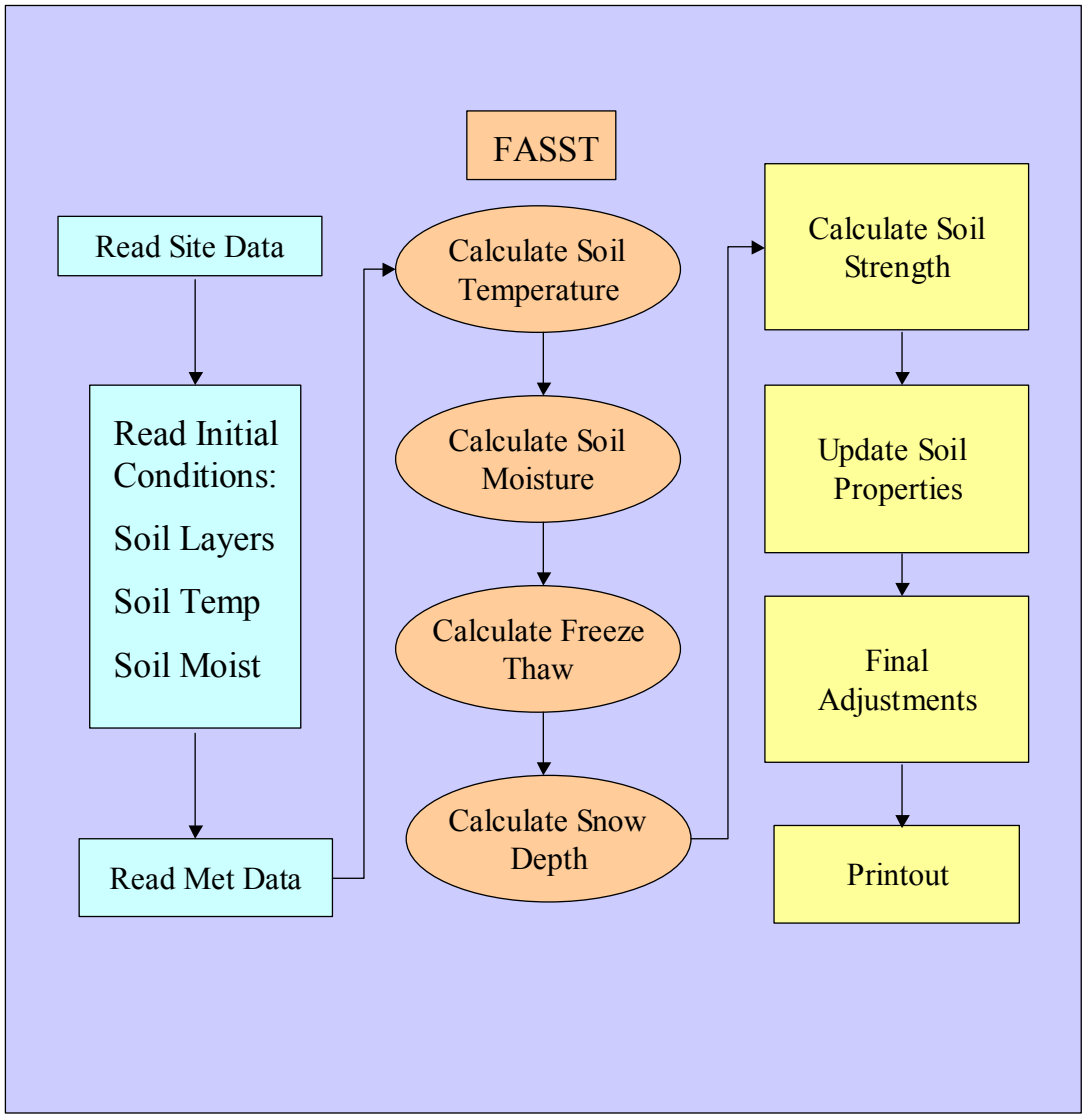

Figure 3.2. FASST flow chart.

CHAPTER 4. METHODS AND MEASUREMENTS

4.1. FIELD METHODS

Monthly snowpits were excavated at the main meteorological towers to obtain the snowpack characteristics, which included snow depth, snow profile temperatures and density taken every 10 cm from the snow surface to the base of the snowpack and snowpack layer height and associated snow grain size and type. This snow information from Illinois River and Buffalo pass served as the snowpack nodal information and soil layer data that were required to initialize SNTHERM and FASST respectively (Tables 4.1 - 4.4).

Table 4.1. SNTHERM initial conditions for Buffalo Pass.

Buffalo Pass Initial Conditions for SNTHERM, March 29th, 1200 MST 2003				
Node	Node height (m)	Kelvin	Density (kg/m$^{3)}$	Grain size (m)
1	0.137	271	416	$1.1X10^{-4}$
2	0.137	271	416	$1.1X10^{-4}$
3	0.137	271	416	$1.1X10^{-4}$
4	0.137	271	416	$1.1X10^{-4}$
5	0.137	271	416	$1.1X10^{-4}$
6	0.137	271	416	$1.1X10^{-4}$
7	0.137	271	416	$1.1X10^{-4}$
8	0.137	271	416	$1.1X10^{-4}$
9	0.137	271	416	$1.1X10^{-4}$
10	0.137	271	416	$1.1X10^{-4}$
11	0.43	269	346	$0.3X10^{-4}$
12	0.43	269	346	$0.3X10^{-4}$
13	0.04	268	297	$0.4X10^{-4}$
14	0.21	268	273	$0.3X10^{-4}$
15	0.01	267	252	$0.3X10^{-4}$
16	0.25	265	194	$0.3X10^{-4}$
17	0.24	271	84	$0.8X10^{-4}$
18	0.01	271	84	$0.8X10^{-4}$
19	0.01	271	84	$0.8X10^{-4}$

Table 4.2. SNTHERM initial conditions for Illinois River.

Illinois River Inital Conditions for SNTHERM, February 21, 1100 MST 2003				
Node	**Node height (m)**	**Kelvin**	**Density (kg/m$^{3)}$**	**Grain size (m)**
1	0.02	270	184	$9.5X10^{-4}$
2	0.03	272	184	$9.5X10^{-4}$
3	0.02	272	184	$9.5X10^{-4}$
4	0.01	272	184	$4X10^{-4}$

Table 4.3. FASST soil initial conditions for Buffalo Pass.

Soil Layer Data used as Initial Conditions for Fasst at Buffalo Pass March 29th, 2003					
Depth (m)	**Snow Depth (m)**	**Soil Moisture (m^3/m^3)**	**Soil Temperature (^oC)**	**Soil Type**	**Layer Thickness (m)**
0	3	------	1	OH	n/a
0.05	------	0.58	1	OH	n/a
0.20	------	0.57	1	OH	n/a
0.50	------	0.61	2	OH	0.50

Table 4.4. FASST soil initial conditions for Illinois River.

Soil Layer Data used as Initial Conditions for Fasst at Illinois River March 14th, 2003					
Depth (m)	**Snow Depth (m)**	**Soil Moisture (m^3/m^3)**	**Soil Temperature (^oC)**	**Soil Type**	**Layer Thickness (m)**
0	0	------	5	OH	n/a
0.05	------	0.35	1	OH	n/a
0.20	------	0.36	1	OH	n/a
0.50	------	0.35	1	OH	0.50

Data used in this study were collected from the fall of 2002 through the snowmelt season in the spring of 2003 on ten-minute intervals (Table 4.5). The CLPX weather stations recorded continuous air temperature, relative humidity, wind speed and direction, incident and reflected solar radiation, upwelling and downwelling longwave radiation, net allwave radiation, soil moisture, soil temperature, snow depth and snow temperature profiles.

Table 4.5. CLPX Instrument specifications and resolution.

Observation	Height (with respect to ground)	Accuracy (manufacturer specified)	Instrument
Wind speed	2 to 4m	±2%	R. M. Young Wind Monitor 05103
Wind direction	2 to 4m	±5°	
Air temperature	2 to 4m	±0.5°C	Vaisala HMP45C
Air relative humidity	2 to 4m	±3%	
Snow depth	2 to 4m	+/- 1cm	Judd Communications Depth Sensor
Incoming and Outgoing Solar and Far Infrared Radiation	10m	+/- 10% (daily totals)	Kipp and Zonen CNR 1 Net Radiometer
Net Radiation	10m	+/- 20%	Kipp and Zonen NR Lite Net Radiometer
Soil moisture	-5cm -20cm -50cm	+/- 0.03 water fraction by volume	Stevens Vitel, Inc. Hydra Probe
Soil Temperature	-5cm -20cm -50cm	+/- 1°C	Type T (Copper Constantan) Thermocouple Wire
Atmospheric Pressure	2 to 4m	+/- 6 mb	Vaisala PTB101B Pressure Transmitter

Stevens Vitel soil probes continuously recorded soil temperature and soil moisture at the soil surface, 0.05m, 0.20m, and 0.50m below the soil surface. These probes also measured the ice content of the soil, which is beyond the scope of this paper. The soil types for each field site were measured from soil surveys.

Snow depth, density, grain size and temperature profiles were obtained during CLPX and from the monthly snowpits that were excavated at the center of each ISA. A continuous record of snow depth at each site was obtained from the acoustic depth sensor, which records the distance from the instrument to the surface (snow or bare ground) in meters. This distance was subtracted from the measured instrument height to obtain snow depth. To find more details regarding the field and remote sensing methods during the CLPX, the reader should refer to (Cline et al., 2003).

The snowpit data and the micrometeorological time series data from the two chosen CLPX study sites will be used to compare the predictions of SNTHERM and FASST.

4.2. MODELING METHODS

SNTHERM has been shown in former studies to accurately predict snowpack characteristics such as snowpack ablation (Rowe et al., 1995; Hardy et al., 1998; Groffman et al., 1999; Gustafsson et al., 2001), but unlike FASST, SNTHERM does not accurately model soil moisture recharge (Jordan, 1991; Frankenstein, 2003). SNTHERM and FASST have not been used to predict snow cover depletion and soil moisture recharge at the NASA CLPX field sites.

SNTHERM was initialized with snowpit layer data during the accumulation season for each field site and driven with the continuous meteorological data to produce continuous snow depth simulations. The Buffalo Pass accumulation season was estimated by examining the plot of the snow depth at each site, during the period where the majority of increases in snow depth occurred. The Buffalo Pass melt season was defined by the period in which few to no increases, but primarily decreases in snow depth occurred (Figure 4.1). Illinois River did not have a discernible pattern to distinguish between the accumulation and melt seasons. Therefore, the results were divided into periods where the model performed with differing modeling accuracy such as over versus underpredictions (Figure 4.2).

Initial conditions for the SNTHERM are listed in Tables 4.1 - 4.2. SNTHERM reads the snowpack layer data from the ground to the snow surface. The observed snow layer thicknesses were divided into smaller sub-layers so that SNTHERM would not over predict the mass balance (Tables 4.1 - 4.2). The snow depth predictions from SNTHERM were compared to the observations for each site throughout the melt season.

SNTHERM will not allow precipitation at the initial time step. If precipitation occurred at the beginning of the model runs, the precipitation amount was added to the following time step. This situation occurred at the Buffalo Pass site.

FASST snow depth simulations were also analyzed. The only initial condition requisite for this prediction was the snow depth at the initial time step. This simulation did not require a separate model procedure from the soil moisture prediction requests. The model generates several output files including snow depth, soil moisture and temperature and meteorological predictions following every model run.

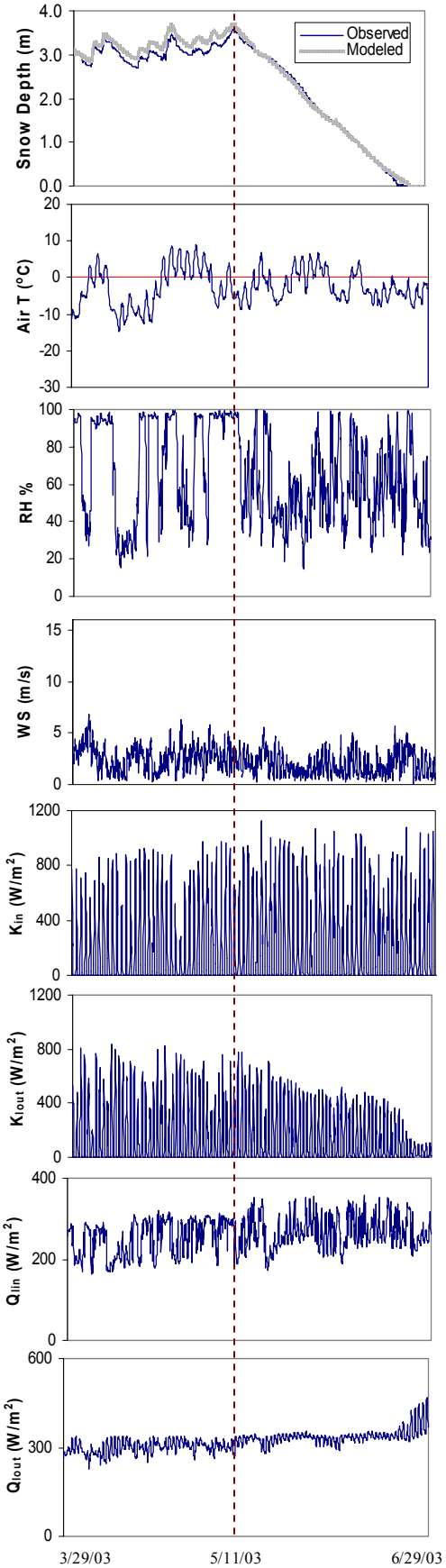

Figure 4.1a-h. Buffalo Pass Meteorological conditions and SNTHERM snow depth results in the following order: a. snow depth, b. air temperature, c. relative humidity, d. windspeed, e. incoming shortwave radiation, f. outgoing shortwave radiation, g. incoming longwave radiation and h. outgoing longwave radiation. The dashed line separates period 1 (accumulation) from period 2 (melt).

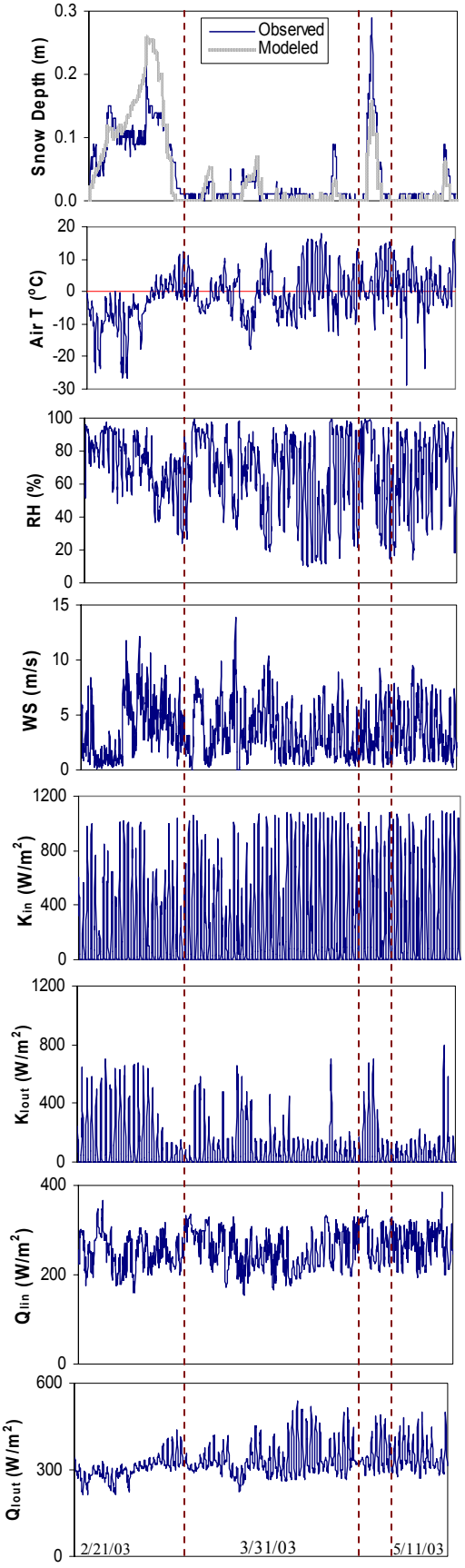

Figure 4.2 a-h. Illinois River Meteorological conditions and SNTHERM snow depth results in the following order: a. snow depth, b. air temperature, c. relative humidity, d. windspeed, e. incoming shortwave radiation, f. outgoing shortwave radiation, g. incoming longwave radiation and h. outgoing longwave radiation. The dashed line separates periods of differing modeling accuracy.

FASST was initialized with soil layer moisture and temperature values (Tables 4.3 - 4.4) and was driven by the continuous meteorological parameters to produce continuous soil moisture simulations. The FASST soil moisture predictions were compared to the observations during the same time frame as the SNTHERM snow depth simulations for Buffalo Pass, but a slightly shorter time frame as the SNTHERM snow depth simulations for Illinois River because of a model coding difficulty with large temperature variations between single time steps. For Buffalo Pass, the FASST default soil type of organic sand, silt and clay (OH) was used as the initial condition to a depth of 0.50m. The FASST default soil type of organic sand, silt and clay (OH) was also used to a depth of 0.50 m at Illinois River. FASST assumes the bottom layer soil type extends to a depth of 1.0m below the soil surface. These FASST default soil types were chosen since they most closely represented the soil survey data hydraulic properties (Frankenstein, 2003).

A sensitivity analysis was performed with both models by adjusting the meteorological parameters for SNTHERM, and soil properties for FASST in order to explore the effects on snow depth and soil moisture predictions. Percent changes were calculated to quantify the model performance after the modifications were made to the input parameters.

4.3. ANALYSIS METHODS

4.3.1. Data Management

For the ISA's at Buffalo Pass and Illinois River, the meteorological parameters, snow depth, snow temperature profiles, soil temperature and soil moisture measurements were arithmetically averaged over an hourly interval to be used in the model simulations.

The time series snow depth data and the snowpit depth data were not identical for any of the field sites, which could be due to the hourly averages of the depth values or the fact that the snowpit was not excavated in the exact location as the acoustic snow depth instrument. Therefore, the snowpit depths were scaled down such that the snowpit depth matched the time series snow depth data. The scaling procedure consisted of dividing the thickness of each snowpack layer by the total snowpack depth. This ratio multiplied by the snow depth measured from the acoustic snow depth instrument served as the new snow depth value.

Single missing data points from the averaged data set were estimated by calculating the arithmetic mean of the previous and subsequent points. Consecutive missing data points were estimated from a linear regression equation calculated from the previous and subsequent three data points. If three data points were not available because they were also missing, then one point before and one point after the missing data was used to calculate the linear regression equation. Neither of these methods was applied if the observed data before and after the missing data were the identical value. In this case, the unchanged value was used in place of missing data. Erroneous data values were treated as missing observations in order to estimate a representative value. If observations

were recorded from the instrumentation that were less than the instrument resolution, the smallest value that fit the resolution criteria was used (Table 4.5).

Precipitation gauges were installed at both sites. However, the precipitation gauge at Buffalo Pass did not function properly. Therefore, precipitation data for Illinois River and Buffalo Pass were estimated from the original snow depth data. The increase in snow depth at each time step was converted to a depth of water by assuming the snow depth to water ratio was 10 percent at Buffalo Pass. This ratio was used because the chosen modeling period was predominantly during the spring melt period, when the new snow density is higher than during the cold, dry winter season. At Illinois River during February 21 through March 13, the average temperature was less than $-5^{o}C$. Therefore, 6 percent water content of precipitation was assumed. For the rest of the season at this site, 10 percent water content of precipitation was assumed since the average temperature was above $0^{o}C$.

For the snowpit data collection protocol, two density samples from every 0.10 m were measured. The average of these two measurements was calculated and used as the initial density for each individual layer (node in SNTHERM). The medium snow grain value used in SNTHERM was obtained by averaging the length and width of the snow grain that was measured in the field. These two values were averaged to obtain one value for the grain size within each node to be used as an initial grain size condition for SNTHERM.

4.3.2. Model Analyses

The results from SNTHERM and FASST were plotted along with the observations for each field site. Periods with differing modeling accuracy were examined closely in conjunction with the meteorological variables and knowledge of the field sites in order to conclude reasons for model error. A brief sensitivity analysis was performed with both models to explore the model's predictive abilities when observed variables were altered. The meteorological radiation parameters were altered to analyze SNTHERM's prediction of snow depth. Soil properties were altered to analyze FASST's estimation of soil moisture evolution.

SNTHERM and FASST snow depth simulations were considered "accurate" if the simulations replicated the observed pattern (timing) of snow depth evolution and if the absolute and relative error rates were less than 20%. An accurate range of the estimated snow cover depletion date was defined as within 5 days of the observations.

FASST volumetric soil moisture simulations were defined as accurate if the seasonal predicted values did not exceed the observations by more than the absolute value of 0.30 m^3/m^3 and the error rates were less than 20%. Soil moisture recharge estimations were accurate if the model mirrored any of the observed increases (timing) in soil moisture at any of the three depths for each site.

4.3.3. Statistical Analyses

Observed versus modeled plots were also utilized to analyze the model accuracy. A 1:1 line was plotted to visually represent the over or underpredictions made by the

models. The closer the points were relative to this line, the fewer discrepancies existed between the observations and the modeled values.

Absolute and relative error calculations were made in an effort to explain both model performances. The absolute error rate shows how well the model predictions fit to the observations during the chosen modeling period. The relative error rate quantifies the discrepancy between individual observed and modeled data points.

4.4. OBJECTIVES

The objectives of this research were to test the ability of SNTHERM and FASST, to predict site-specific snow cover depletion and underlying soil moisture recharge by using the CLPX data.

CHAPTER 5. RESULTS

5.1. METEOROLOGICAL CONDITIONS

5.1.1. Buffalo Pass

The meteorological data used to drive SNTHERM and FASST are shown in Figures 4.1a-h. The air temperature (Figure 4.1b) and the relative humidity (Figure 4.1c) show different patterns during the accumulation period (March 28 - May 9) than during the melt period (May 10 – June 24). The range of variability in the air temperature was much greater during the accumulation period than during the melt period.

There were several occasions where the relative humidity reached 100% for consecutive days. As the melt season began, the relative humidity pattern underwent a dramatic change. The graph suggests that the average values of humidity were much lower during the melt season than the accumulation season. The humidity reached 100% during the melt season, but dropped quickly thereafter. The humidity fluctuated from day to day, unlike the previous season when the humidity was more constant.

Figure 4.1d shows the changes in the wind speed patterns are not as pronounced from season to season as the fluctuations in air temperature and relative humidity. The wind speed was generally lower and slightly less variable during the melt season than during the accumulation period.

The values of incoming shortwave radiation were overall lower during the accumulation period than during the melt period. It is clear that within periods where the relative humidity was near 100%, the incoming shortwave radiation was less than 600

W/m^2 (Figure 4.1e). This scenario suggests that clouds were present and precipitation was occurring.

The outgoing shortwave radiation was much greater during the accumulation season than during the melt season as shown in Figure 4.1f. This situation shows that the snowpack absorbed more incoming shortwave radiation during the melt season, which contributed to the melting snow.

The longwave radiation data in Figure 4.1g-h does not vary much from season to season. The graph of incoming longwave radiation shows a slight overall increase during the melt season compared to the accumulation period. The outgoing longwave radiation became slightly less variable for the majority of the melt season than the preceding season. The outgoing longwave radiation remained a fairly steady 300 W/m^2 until the concluding stages of the modeling period, when the vegetation was exposed and the outgoing longwave radiation increased to 400 W/m^2.

5.1.2 Illinois River

Figure 4.2a-h contains the plots of the meteorological variables used for SNTHERM and FASST modeling periods. The range of variability of each meteorological plot was much greater than the range of variability of the Buffalo Pass plots. The variable meteorological data created a difficult modeling environment.

Throughout the modeling period (February 21 – May 11), the air temperature gradually warmed to reach 0^oC and was well above 0^oC near the end of the period. During February 21 – March 12 (period 1) when the model overpredicted the snow depth, the air temperature was well below 0^oC until March 1 as the temperature slowly began to

increase to 0^{o}C point by March 7. March 1 is also the day that the simulated snow depth began to noticeably diverge from the observations. The next period (period 2) where the model underpredicted the snow depth, April 22 – April 26, the air temperature steadily increased to well above 0^{o}C, then began to drop drastically to well below 0^{o}C by May 1. After this day, the air temperature increased to above 0^{o}C (Figure 4.2b).

The values of relative humidity were near 100% on February 21, and then declined until March 13. After March 13, the humidity generally increased until March 16. Outside this period, there was no discernible pattern except that the humidity was highly variable. The humidity dropped from near 100% to near 10% most days during the chosen modeling period (Figure 4.2c).

The wind speed was highly variable during the entire modeling period. During period 1 on March 1, the wind speed increased from 0.5m/s to 8m/s. Following March 1, the range of variability of the wind speed increased (Figure 4.2d).

Figure 4.2e shows that the incoming shortwave radiation showed smaller values during period 1 than the rest of the modeling period indicating that cloud cover was present. The rest of the modeling period shows short periods where the incoming shortwave radiation was low.

The outgoing shortwave radiation plot illustrates the fact that snow cover at this site is short lived. Less shortwave radiation is absorbed when the snow is on the ground due to its high albedo. During period 1, the outgoing shortwave radiation is high, and then dropped gradually from 675 W/m^2 on March 5 to 129 W/m^2 by March 11 as the snow began to melt. At times when the soil and vegetation were exposed, the outgoing

shortwave radiation remained around 150 W/m^2 and increased to around 600 W/m^2 when the snow completely covered the site (Figure 4.2f).

The longwave radiation plots were the least variable of the meteorological parameters at Illinois River during the modeling period. The outgoing longwave radiation showed little variation when the snow covered the ground during period 1. For the rest of the modeling period, the outgoing longwave radiation was more dynamic when patches of the ground were exposed (Figure 4.2g-h).

5.2. SNOW DEPTH

5.2.1. Buffalo Pass

5.2.1a. SNTHERM

Results from SNTHERM at Buffalo Pass during March 28 – June 26 show an excellent fit to the observed snow depth. The model has more trouble accurately predicting the snow depth during the period 1 than during the period 2. Figure 5.1 shows that the model accurately predicted the timing of positive and negative changes in snowpack depth during the accumulation period, but the results were overpredicted by a relatively consistent amount. SNTHERM also predicted the inflection from the accumulation period to the melt period concurrently with the observations on May 9, but still slightly overpredicted the magnitude of the snow depth.

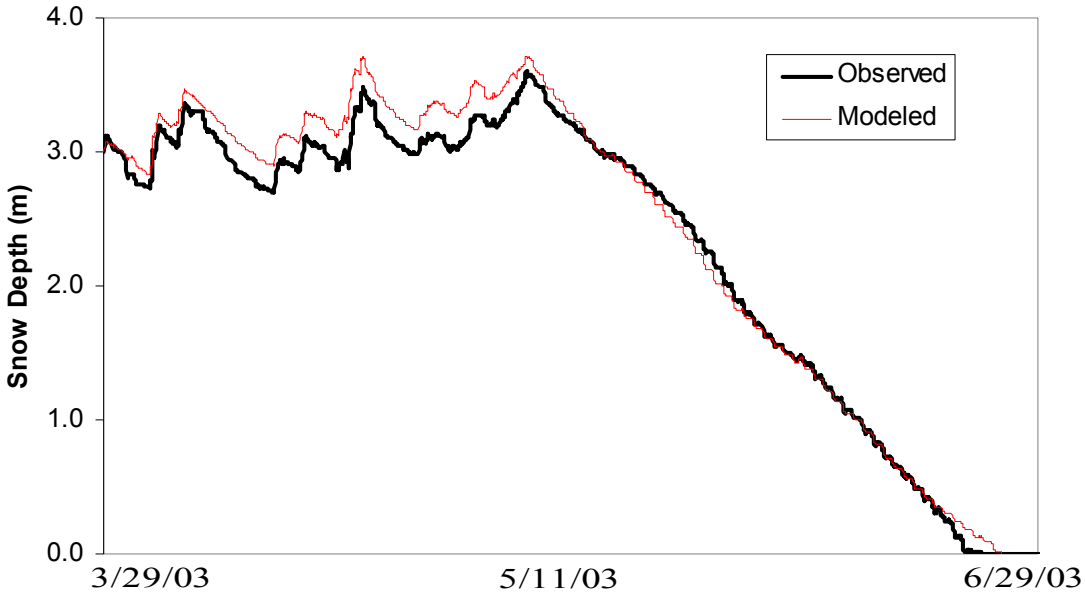

Figure 5.1. SNTHERM Buffalo Pass results.

Conversely, during the melt period, there was very little discrepancy between the observed and modeled snow depth. The model continued to overpredict the snow depth five days into the melt period. The amount at which SNTHERM overpredicted the snow depth during these five days was small compared to the overpredictions made during the accumulation period. A slight divergence of modeled and observed snow depth occurred between May 21 – June 2 as the model slightly underpredicted the snow depth, which is shown in Figure 5.2. The model did capture the diurnal melt-freeze cycles as shown in Figure 5.3. SNTHERM also overpredicted the snow depth during the last four days that the snowpack was on the ground. However, the simulated snow cover disappearance date (June 26) was only delayed two days past the observations (June 24).

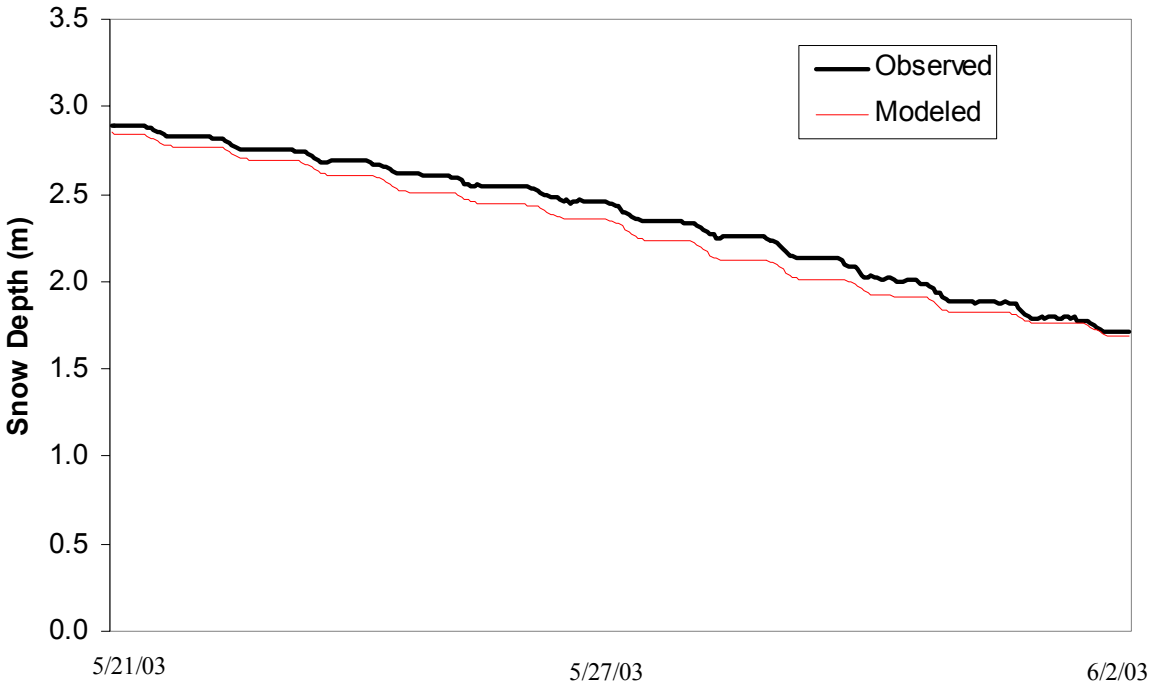

Figure 5.2. Period in which SNTHERM underpredicted snow depth at Buffalo Pass.

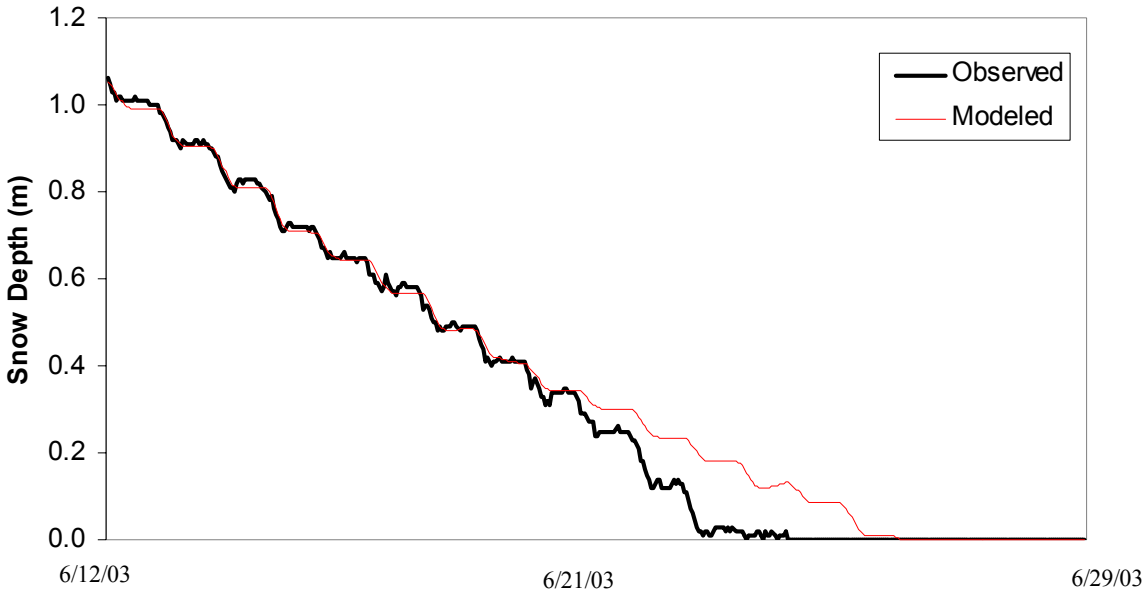

Figure 5.3. Diurnal melt-freeze cycles reproduced by SNTHERM at Buffalo Pass.

Absolute and relative error calculations on Table 5.1 show that the SNTHERM is capable of predicting snow depth at this site despite the over and underpredictions made by the model. The absolute error rate was only 11%, which illustrates that the overall fit of the model was excellent. The relative error rate was 5%. This small relative error rate shows that the model performs well relative to the individual observations.

Table 5.1. SNTHERM absolute and relative error rates at Buffalo Pass and Illinois River.

Error Rates of Modeled Snow Depth		
Sites:	Buffalo Pass	Illinois River
Absolute	11%	2%
Relative	5%	43%

Figure 5.4 is a scatter plot of observations and modeled snow depth relative to the 1:1 line. This plot shows that most of the discrepancy occurs at depths below 0.35m and above 2.6m. These discrepancies are above the 1:1 line, which indicates that the model overpredicted the snow depth. Some of the points lie below the line at depths approximately between 1.6m and 2.7m. SNTHERM displayed fewer discrepancies between approximate snow depths of 0.30m and 1.6m.

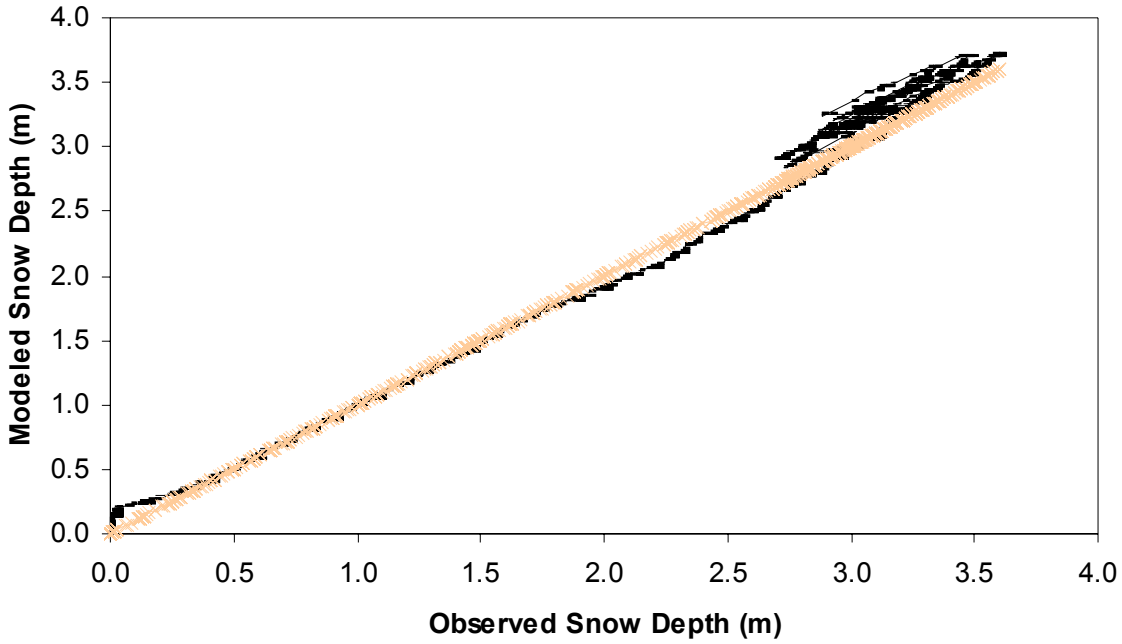

Figure 5.4. Scatter Plot of Buffalo Pass snow depth observations and SNTHERM modeled results with a 1:1 line.

5.2.1b. FASST

FASST snow depth results were in excellent agreement with the observations (Figure 5.5). The timing of snow changes, the magnitude of snow depth and the snow cover depletion date show very little mistakes were made in the estimations produced by FASST. Figure 5.6 illustrates the minimal observed and modeled divergence from the 1:1 line at Buffalo Pass. Table 5.2 shows that the relative error rate from FASST at Buffalo Pass was 2% and the absolute error rate was 1%.

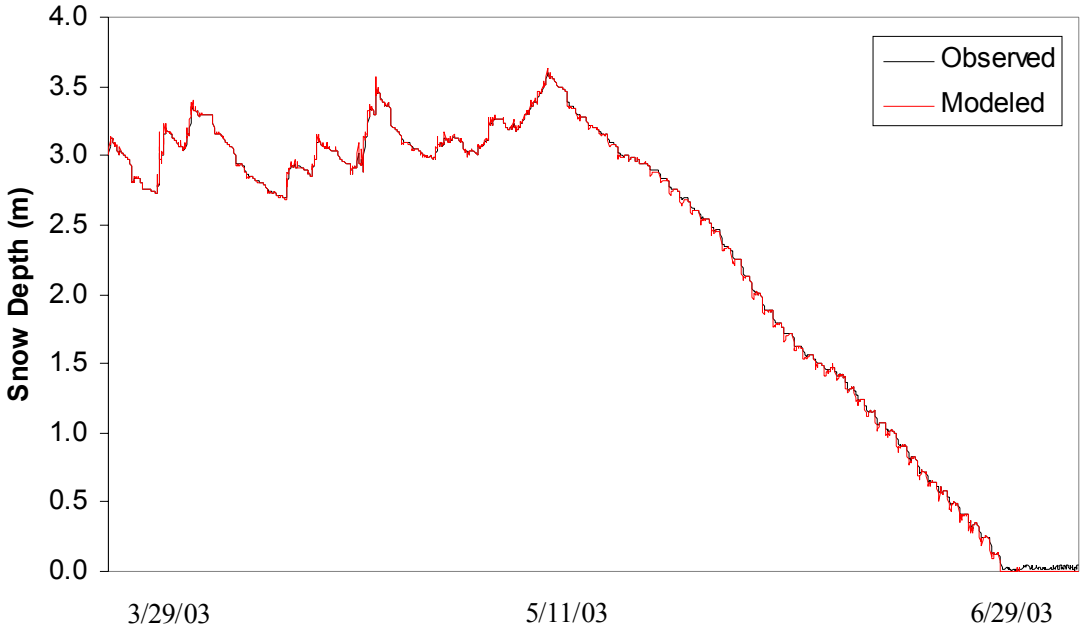

Figure 5.5. FASST snow depth results from Buffalo Pass.

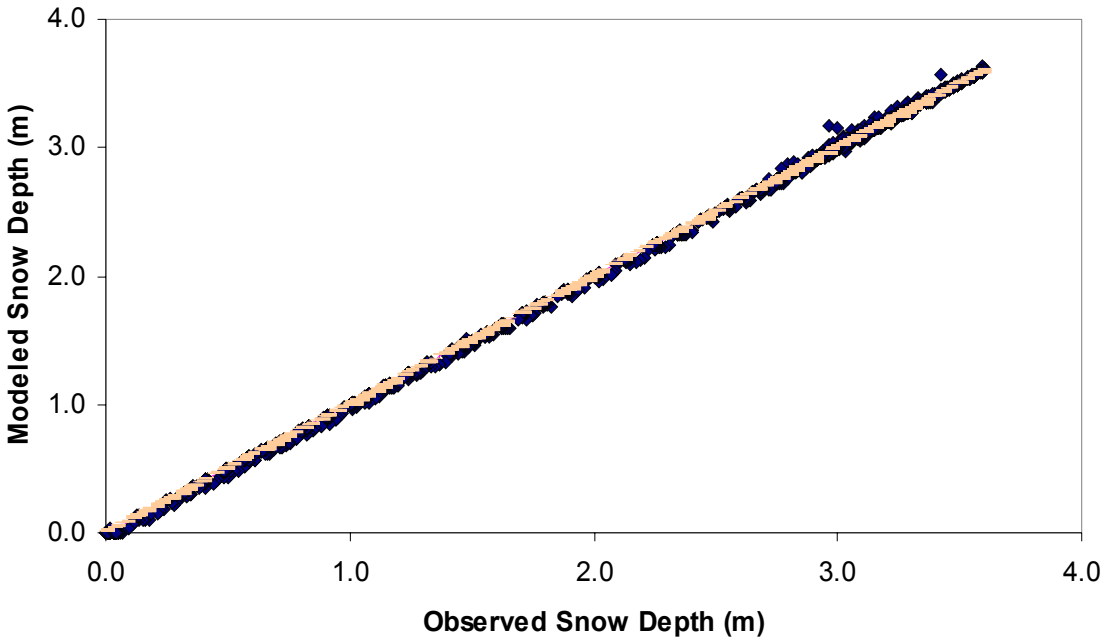

Figure 5.6. Scatter plot of Buffalo Pass snow depth observations and FASST snow depth results with a 1:1 line.

Table 5.2. Relative and absolute error rates from FASST snow depth results at Buffalo Pass

FASST Relative and Absolute Error For Snow Depth Predictions		
Site	Relative	Absolute
Buffalo Pass	2%	1%

FASST predicted the snow depth more accurately than SNTHERM. Figure 5.7 compares FASST and SNTHERM simulated snow depth at Illinois River respectively. Table 5.3 compare the model performance statistics, which shows that SNTHERM has an 11% absolute error rate, while FASST has a 1% absolute error rate. The relative error associated with SNTHERM at this site is 5% and FASST is only 2%.

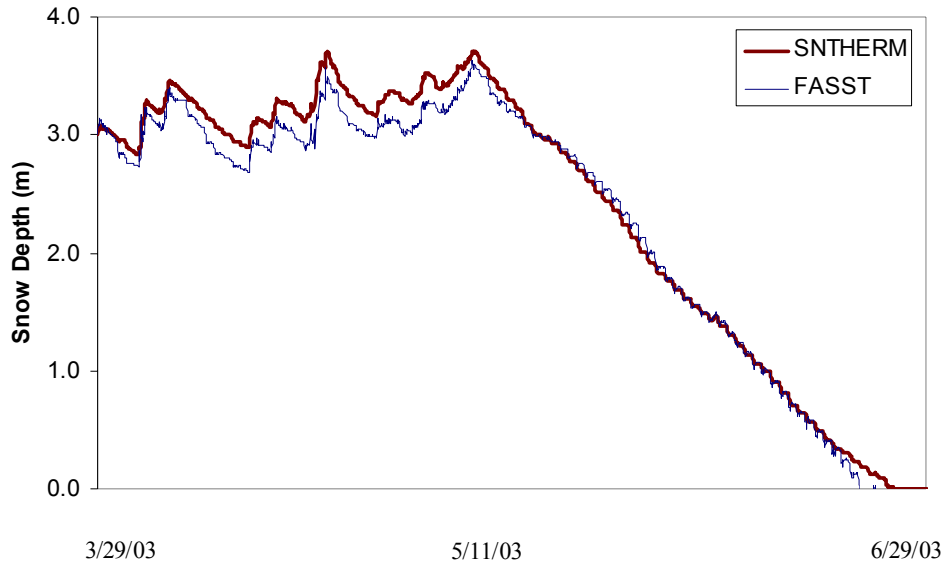

Figure 5.7. Comparison of SNTHERM and FASST simulated snow depth at Buffalo Pass.

Table 5.3. Comparison of SNTHERM and FASST model error rates.

SNTHERM and FASST Relative and Absolute Error From Snow Depth Predictions For Buffalo Pass	
Absolute	Relative
SNTHERM: 11%	SNTHERM: 5%
FASST: 1%	FASST: 2%

The previously discussed snow depth results from FASST utilized the continuous snow depth observations. Figure 5.8 shows new FASST snow simulations, which the continuous snow depth observations were not supplied for the model run. Buffalo Pass new snow depth simulation was overpredicted by over 100%. The simulation predicted the timing of snow depth changes accurately, but the magnitude was the major source of error.

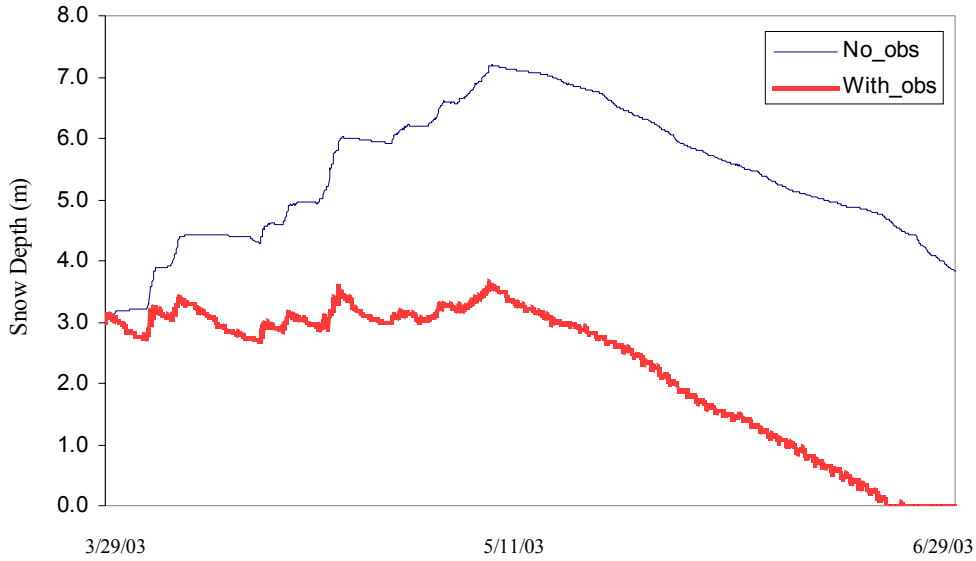

Figure 5.8. FASST snow depth results with continuous snow depth observations and without.

5.2.2. Illinois River

5.2.2a. SNTHERM

SNTHERM snow depth and snow cover depletion date estimations fit the criteria for accurate except for the relative error rate calculation at Illinois River. Figures 4.2 and 5.9 show that the model reasonably predicted the timing of the accumulation and melt throughout the modeling period, February 21 – May 11.

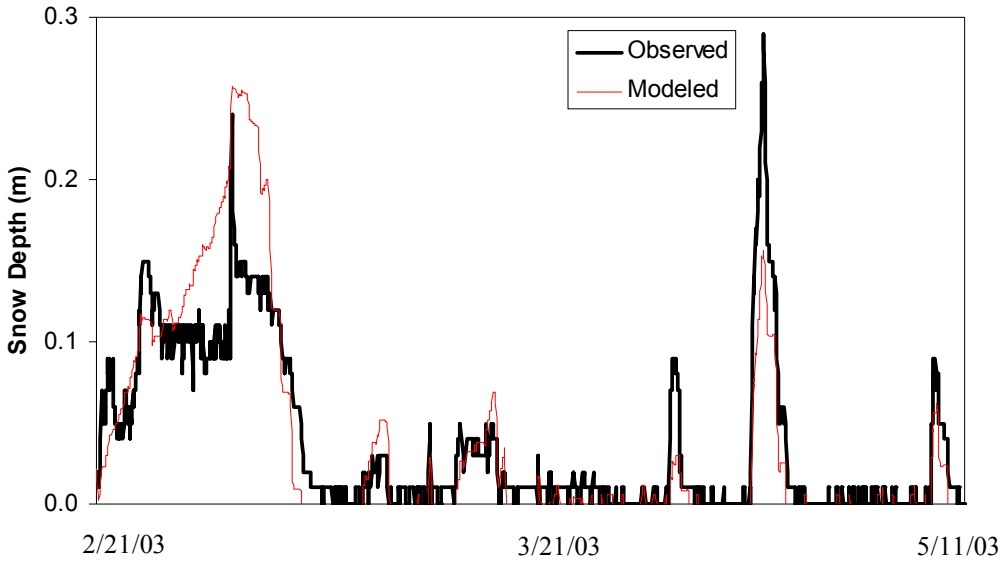

Figure 5.9. Observed and modeled snow depth at Illinois River.

The model had difficulty predicting the magnitude and dynamics, or variability, of snow depth from period 1 and 2. The simulated snow depth during period 1 was overpredicted by a maximum of 0.12m. The simulation did not accurately capture the snow depth dynamics of this period. Instead, the results resemble a smoothed version of

the observations. The modeled results from period 2 captured the dynamics of the snow depth accurately, but underpredicted the snow depth by a maximum of 0.14m.

As a whole, SNTHERM accurately modeled snow depth dynamics, magnitude, and timing associated with smaller storms during the season that produced less than 0.05m of snow. SNTHERM predicted that complete snow cover depletion occurred only one day earlier than the observations.

Absolute error calculations were done to quantify the overall fit of the model and are shown in Table 5.1. Relative error was calculated to determine the percent differences between the modeled and observed snow depth data during periods where the model clearly over or underpredicted the observations. The absolute error rate was 2% and the relative error rate was 43%. This small absolute error rate reveals that the overall fit of snow depth simulations were in excellent agreement with the observations. The relative error calculation shows that regardless of the shallow snow depth, the model has difficulty with modeling the magnitude of snow depth during period 1 and 2.

Figure 5.10 shows the observed versus modeled points relative to the 1:1 line. A discernable pattern regarding the modeled results is not evident. This plot shows that the model over and underpredicted the snow depth observations for a given observed snow depth value. The majority of the variability between the modeled and observed data occurred when the observed snow depth was within the range of 0.07m to 0.25m.

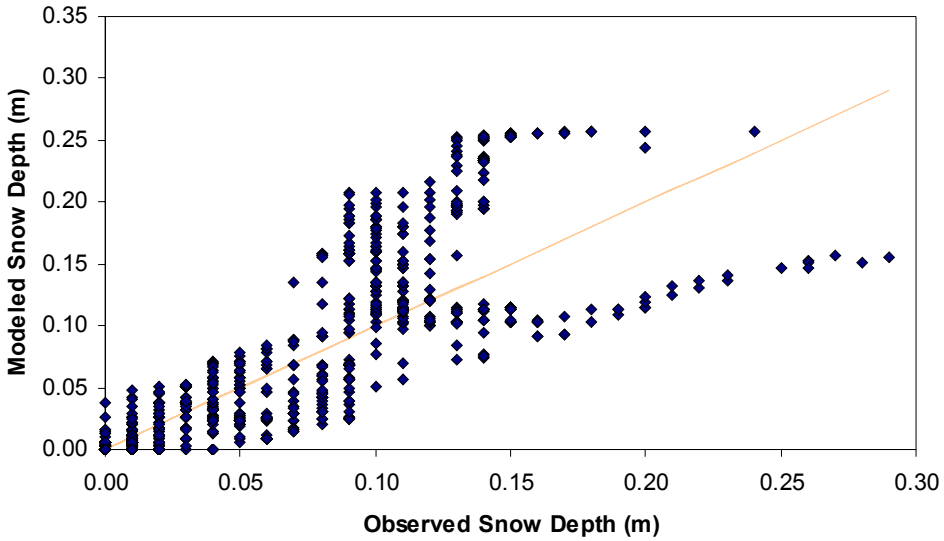

Figure 5.10. Scatter plot of Illinois River observed and SNTHERM modeled snow depth with a 1:1 line.

5.2.2b. FASST

Figure 5.11 shows that FASST predicted the evolution of snow depth at Illinois River in agreement with the observations. Figure 5.12 is a plot of residuals from Illinois River. The residuals vary more than at the Buffalo Pass site, but are within 0.10m or less of the observations. Most of the variability occurred when the snowpack was less than 0.15m deep. Table 5.4 shows that the absolute and relative error rates were both less than 1%.

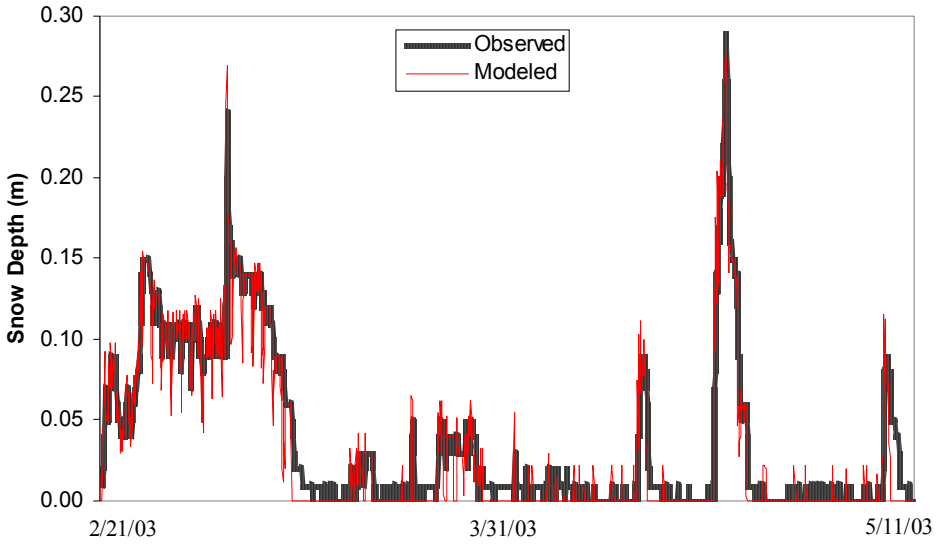

Figure 5.11. FASST snow depth results from Illinois River.

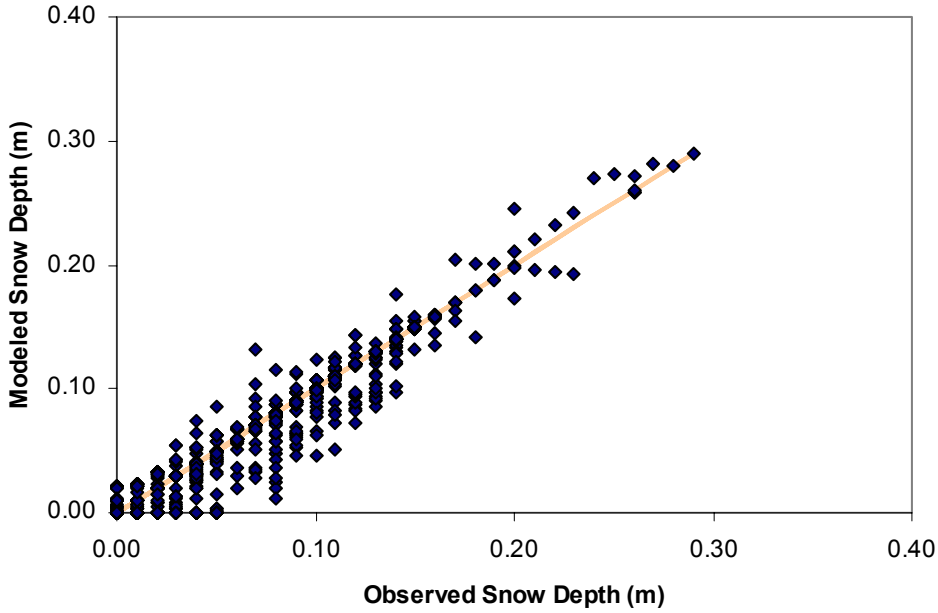

Figure 5.12. Scatter plot of Observed versus FASST modeled snow depth at Illinois River.

Table 5.4. FASST model performance statistics at Illinois River

FASST Relative and Absolute Error For Snow Depth Predictions		
Site	Relative	Absolute
Illinois River	<1%	<1%

FASST predicted the snow depth more accurately than SNTHERM. Figure 5.13 compare plots of FASST and SNTHERM predicted snow depth at Illinois River. Table 5.5 compares the model performance statistics from Illinois River. At Illinois River, SNTHERM has a 2% absolute error rate and FASST has an absolute error rate less than 1%. SNTHERM has a 43% relative error rate and FASST has a relative error rate less than 1% at this site.

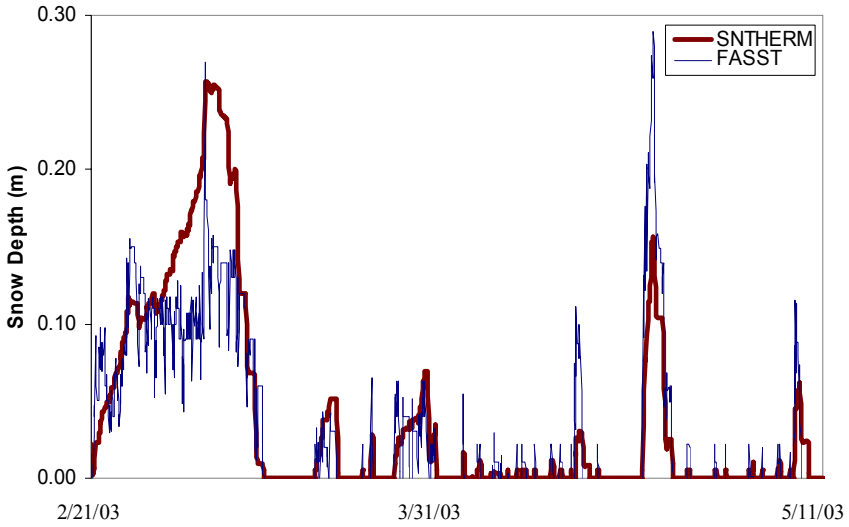

Figure 5.13. SNTHERM and FASST modeled snow depth at Illinois River.

Table 5.5. Comparison of SNTHERM and FASST model performance statistics.

SNTHERM and FASST Relative and Absolute Error From Snow Depth Predictions For Illinois River	
Absolute	Relative
SNTHERM: 2%	SNTHERM: 43%
FASST: <1%	FASST: <1%

The FASST snow depth estimations used the continuous snow depth observations. Figure 5.14 shows that without using the snow depth observations, FASST overpredicted the snow depth by 4.5%. The simulations predicted accurate timing of snow depth changes, but the snow depth magnitude estimation was problematic for FASST.

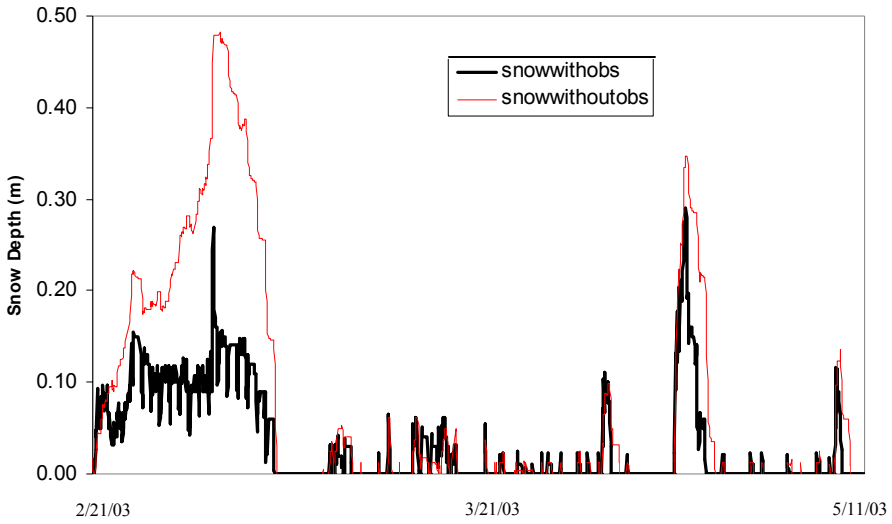

Figure 5.14. Comparison of FASST simulated snow depths with continuous snow depth and without.

5.3. SOIL MOISTURE

5.3.1. Buffalo Pass

Figures 5.15a-c and 5.16a-c show that FASST predicted the soil moisture at Buffalo Pass during March 28 – June 24 similar to the observations. The model predicted more dramatic changes in soil moisture than the observations demonstrate, although the values were still underpredicted. The model predicted the timing of the soil moisture changes at the 0.05 m and 0.20 m levels but not the 0.50 m level. Interestingly, the model accurately predicted that the 0.50 m level had the greatest soil moisture storage out of the three depths, which agreed with the observations. FASST also did not forecast the small diurnal fluctuation of the observations.

FASST underpredicted the soil moisture at the 0.05m level by a maximum of 0.08 m^3/m^3 throughout the entire modeling period (Figure 5.16a). Predicting the microphysics of the soil moisture was problematic for FASST. The model predicted more dramatic changes in soil moisture than the observations show. The modeled 0.05 m soil moisture resembled the peaks and valleys of the observed changes in snow depth (Figure 5.17). For a given peak in snow depth, the 0.05 m soil moisture plot showed a peak within a few days. During the melt season when no snow accumulation occurred, the soil moisture simulation commenced to gradually decrease. Near the end of the modeling period, the observations began to decrease as well. Some of the dynamics of the modeled soil moisture replicated the observed soil moisture. For instance, the model predicted an increase of soil moisture on April 9, which agrees with the observed soil moisture that increased on April 10. The modeled increase was 0.04 m^3/ m^3 less than the observed values.

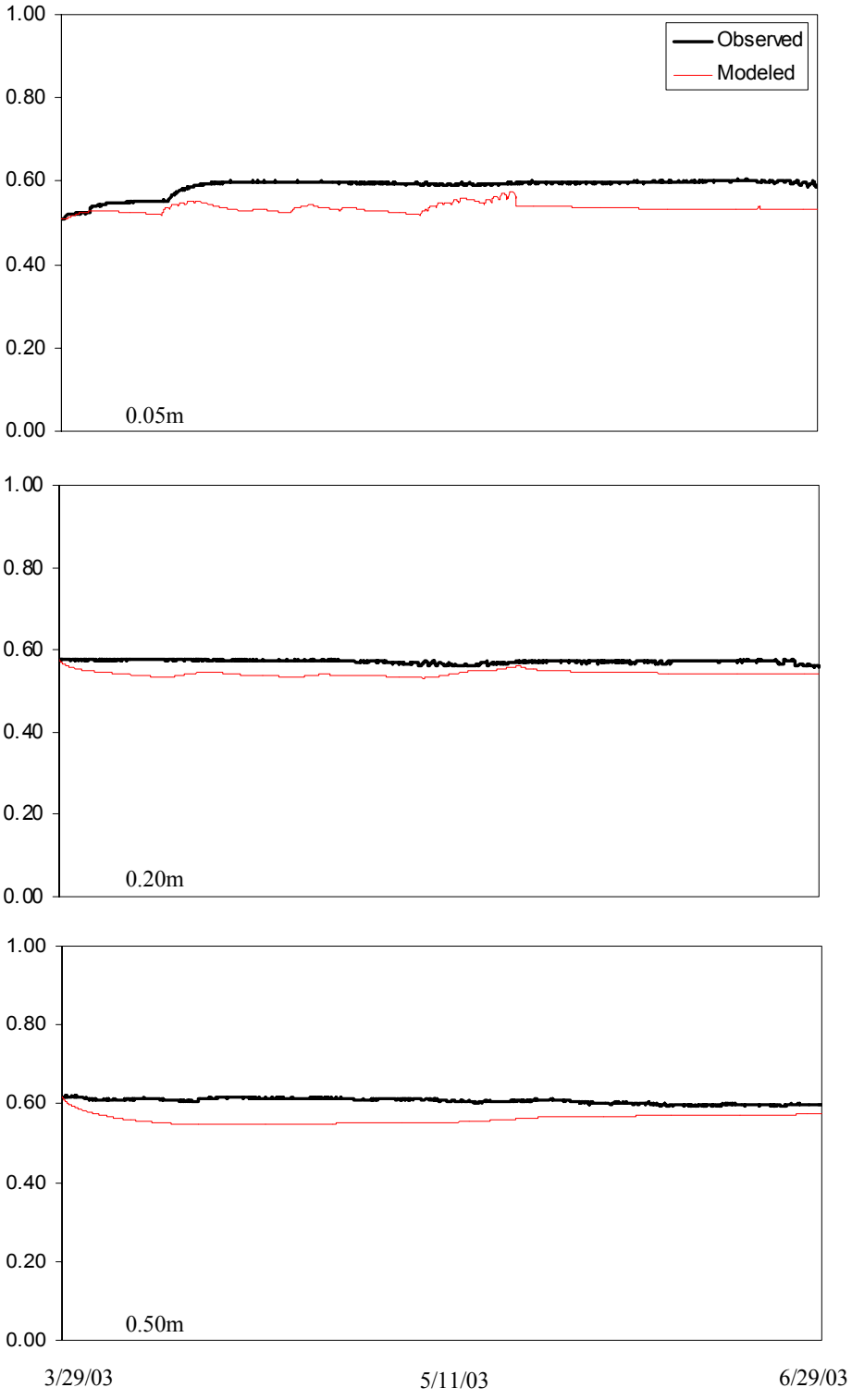

Figure 5.15. a - c. Buffalo Pass observed and FASST modeled soil moisture at: a. 0.05 m, b. 0.20 m, and c. 0.50 m.

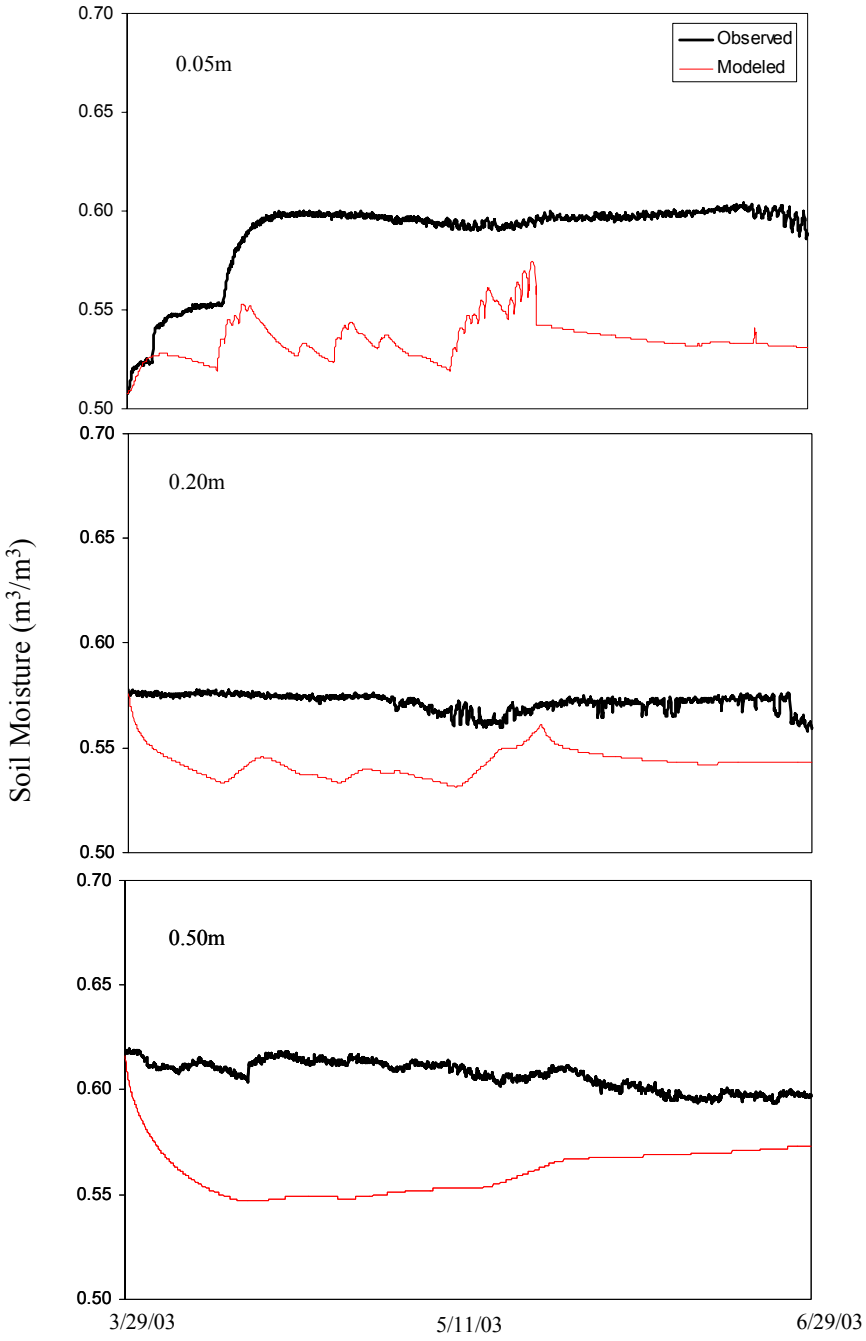

Figure 5.16. a - c. Observed and FASST modeled soil moisture at Buffalo Pass: a. 0.05 m, b. 0.20 m, c. 0.50m.

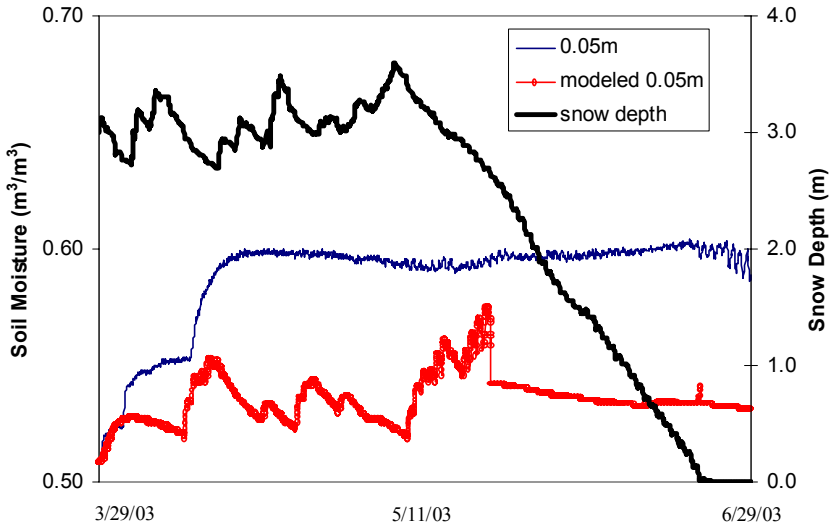

Figure 5.17. Buffalo Pass snow depth observations, observed and modeled 0.05 m level soil moisture.

FASST slightly underpredicted the soil moisture magnitude at the 0.20 m level but predicted a more dynamic soil moisture pattern than the observations show. (Figure 5.16b). The observed soil moisture at this level also exhibited change that corresponded with the observed 0.05 m soil moisture although the values were smoothed and delayed by a few days. On May 18, the observed soil moisture shows a slight increase. The model predicted the increase five days prior to the observations on May 13. Even though the model overpredicted the magnitude of soil moisture increase, the overall value remained less than the observations.

Out of the three depths, the 0.50 m modeled soil moisture was not as accurate as the 0.05 m or the 0.20 m level (Figure 5.16b). FASST continued to underpredict the observed soil moisture at the 0.50m level. The observed soil moisture at this depth decreased during the entire modeling period, but showed more perturbations than the soil

moisture at the 0.05 m and 0.20 m depths. The model predicted a much smoother line and a general trend that increased starting on April 17, while the observations were generally decreasing. The simulation does show a relatively substantial increase in soil moisture on May 15. The observations show an increase five days later on May 20. FASST did predict that the soil moisture at this depth had a greater volume than the other two depths, which agreed with the observations.

The absolute and relative error calculations were done for each soil moisture level and are provided in Table 5.6. These calculations show that the model was capable of modeling the soil moisture accurately at the 0.05 m, 0.20 m and 0.50 m depths below the soil surface. The absolute error rate for the 0.05 m level was only 5%, and the relative error rate was 9%. The absolute error for the 0.20 m level was 3% and the relative error was 5%. The absolute error for the 0.50 m level was 5% and the relative error calculation was 8%.

Table 5.6. Absolute and relative error calculations made to quantify errors made by FASST modeled soil moisture at Buffalo Pass and Illinois River.

FASST Absolute and Relative Error Rates for Buffalo Pass (A) and Illinois River (B)				
(A) Absolute Error	(A) Relative Error	Depths	(B) Absolute Error	(B) Relative Error
5%	9%	0.05m	9%	30%
3%	5%	0.20m	3%	10%
5%	8%	0.50m	9%	34%

Figure 5.18 a - c shows the scattered plots of the observations and modeled soil moisture relative to a 1:1 line at the 0.05 m, 0.20 m and 0.50 m level respectively. These plots illustrate the fact that FASST underestimates the observed soil moisture values at all three depths. Most of the points lie between 0.59 and 0.60 m^3/m^3 at the 0.05 m depth. The majority of the points lies between 0.56 and 0.58 m^3/m^3 at the 0.20m level and reside mostly above the 1:1 line. Much variability exists in the points at the 0.50 m depth. The variability of the residuals in this plot illustrates that no pattern exists between the simulated and the observed soil moisture at this depth.

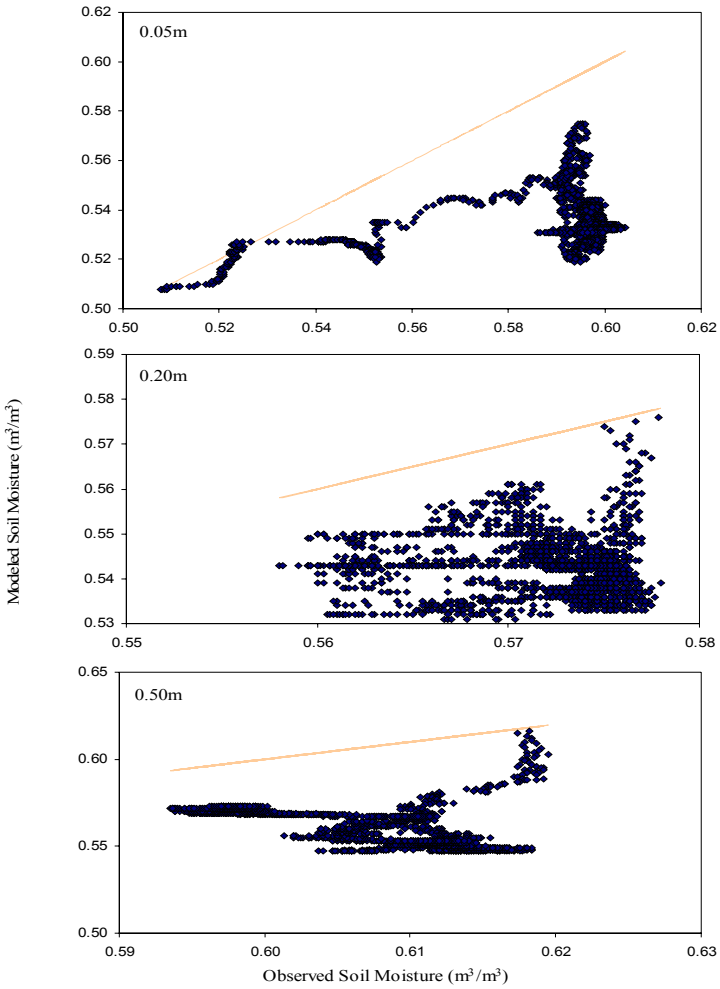

Figure 5.18. a - c. Scatter plots of Illinois River observed and modeled soil moisture with a 1:1 line

5.3.2. Illinois River

The results from FASST at Illinois River are reasonable and are shown in Figures 5.19a-c and 5.20a-c. The model predicted the dynamics and timing of some of the soil moisture changes accurately at this site. On a scale from 0 to 100% possible soil moisture capacity, the model yields a good estimate of the volume of soil moisture at any given time throughout the modeling period (March 13 – May 11).

At the 0.05 m depth the observations show a very dynamic soil moisture pattern even though the model produced results with less perturbations (Figure 5.20a). FASST did capture the timing of soil moisture increases in the latter part of the modeling period. The model overpredicted the magnitude of soil moisture at this level. The simulated results varied less than 0.10 m^3/m^3 from the observations during the entire modeling period.

The observed soil moisture values at the 0.20 m were not as dynamic as the 0.05 m depth. The simulated soil moisture showed the overall increasing seasonal trend of soil the observations. FASST accurately replicated the fact that 0.20 m depth held a greater volume of soil moisture than the other two depths. The model underpredicted the variability of seasonal soil moisture at the 0.20 m level (Figure 5.20b).

The observed soil moisture at the 0.50 m depth echoed the soil moisture variations at the 0.20 m depth, but the magnitude and amount of variability was lower. The modeled soil moisture at the 0.50 m layer but did not capture the dynamic changes in the soil moisture. Both the observations and simulations at this depth illustrate a lower volume of soil moisture storage than the shallower soil depths (Figure 5.20c).

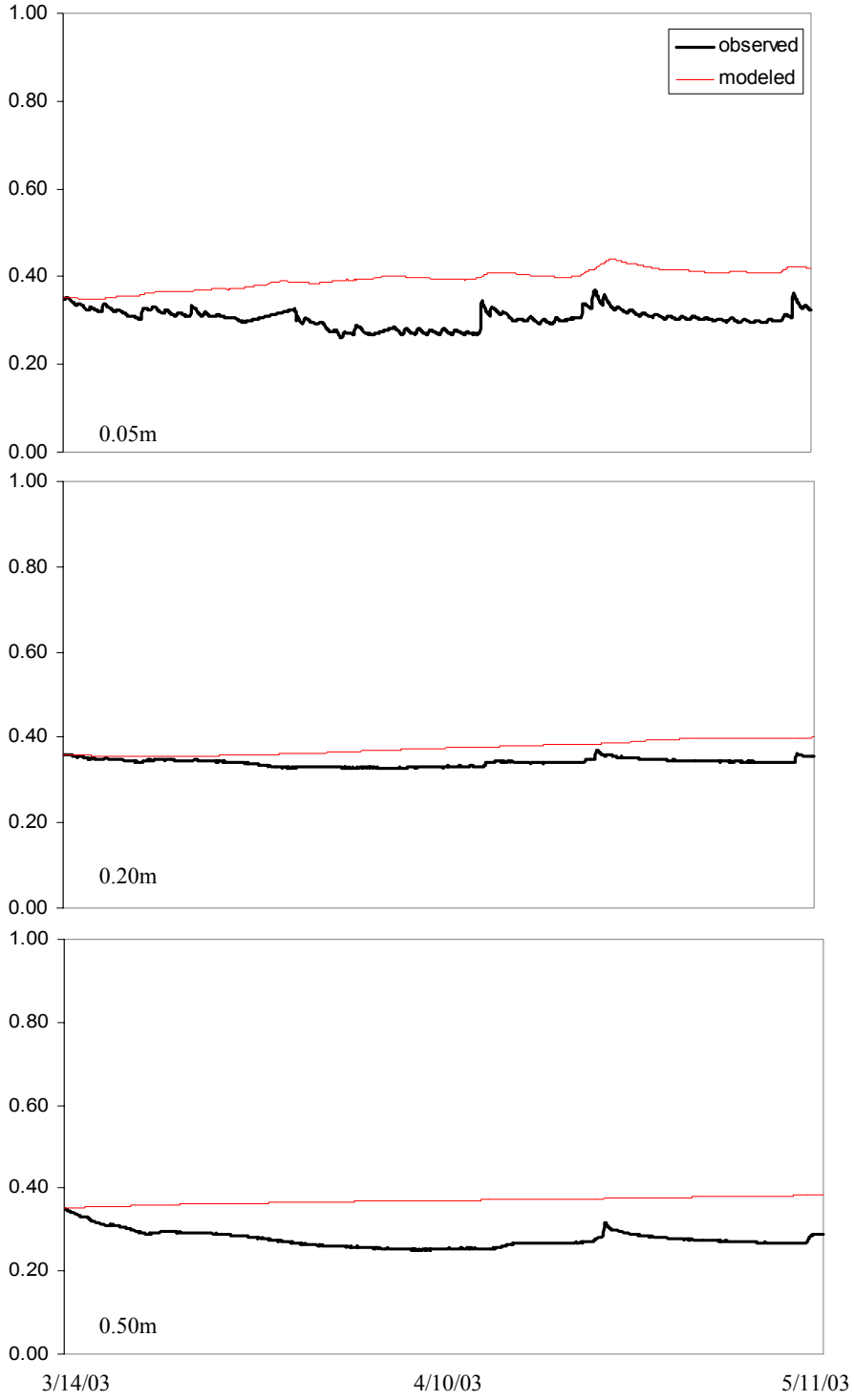

Figure 5.19 a - c. Observed and FASST modeled soil moisture at Illinois River on a scale from 0 to 100% soil moisture capacity.

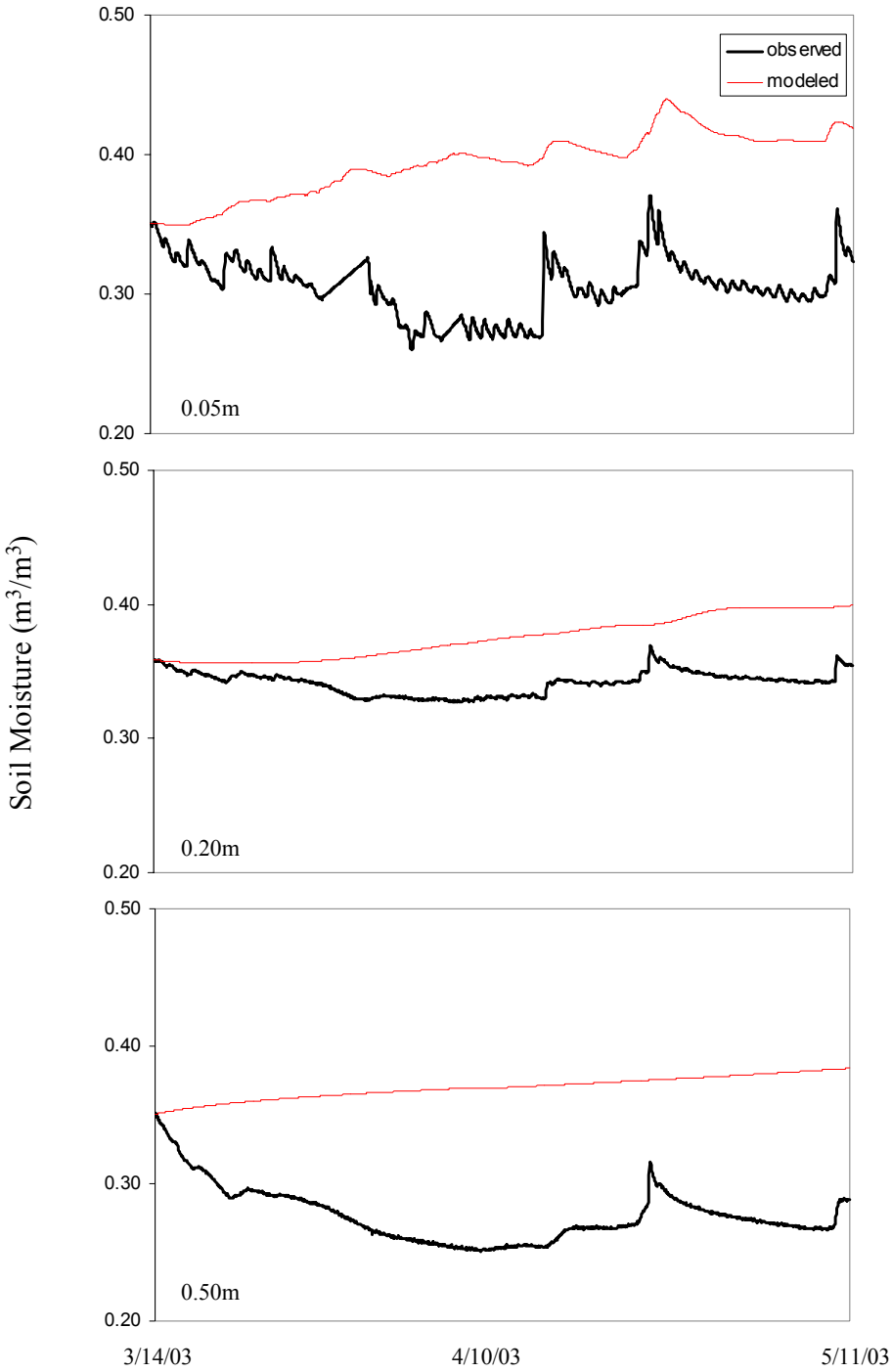

Figure 5.20 a - c. Observed and FASST modeled soil moisture at Illinois River on a refined scale at three depths below the soil surface: a. 0.05 m, b. 0.20 m, c. 0.50 m.

Table 5.6 lists the absolute and relative error calculations of the simulations from FASST. At the 0.05 m, 0.20 m and 0.50 m depths, the absolute error rates were 9%, 3%, and 9% and the relative error rates were 30%, 10% and 34% respectively. The low absolute error rates confirm that the model accurately predicted the evolution of soil moisture values. Conversely, FASST overpredicted the magnitude of soil moisture relative to the observations at the 0.05 m layer and at the 0.50 m layer such that the predictions did not fit the criteria for accurate results.

Figure 5.21 shows the scatter plots at the 0.05 m, 0.20 m and 0.50 m depths. A 1:1 line was plotted on each graph to observe how the points relate to the observations. At the 0.05 m depth, the points show much variability above the line. This plot shows that the model overpredicted the soil moisture. The 0.20 m depth plot show that most of the variability lies above the 1:1 line but reveals that the points fit closer to the line than the other plots. For a given change in the observations, the modeled value remained around a constant value resulting in little predicted changes in soil moisture. The 0.50 m depth residuals show that all of the variability lies above the line for this modeling period. The range of variability occurred between the observed values of 0.25 and 0.35 m^3/m^3.

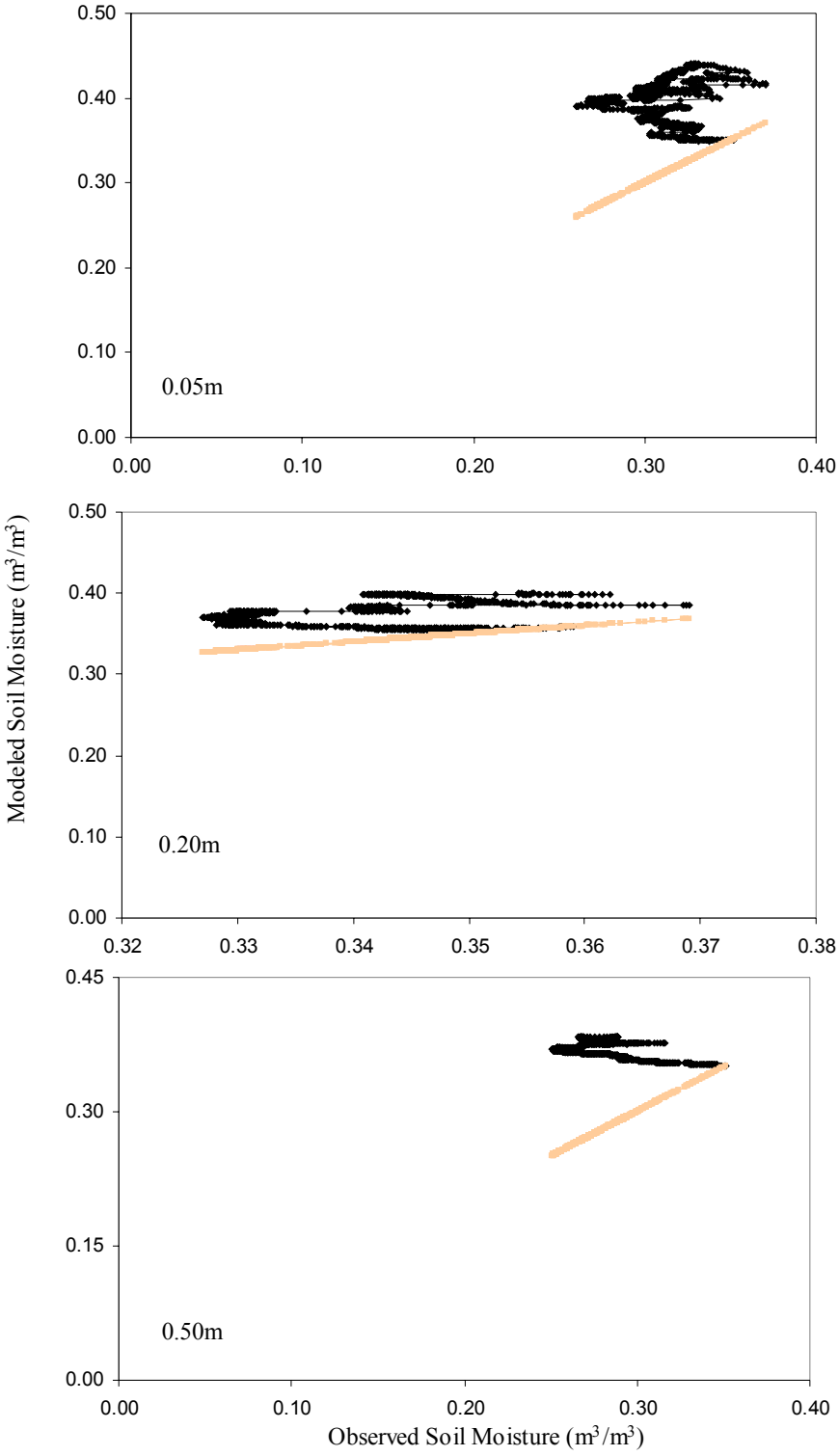

Figure 5.21 a - c. Scatter plots of observed and FASST modeled soil moisture at Illinois River at three depths below the soil surface: a. 0.05 m, b. 0.20 m, c. 0.50 m.

5.4. SENSITIVITY ANALYSIS

5.4.1. SNTHERM

The results from the sensitivity analysis performed using SNTHERM at the Buffalo Pass site show that the predictions of snow depth relied heavily on the meteorological variables. A sensitivity analysis was not explored with the data from the Illinois River site. Both models proved to predict the snow depth and soil moisture more accurately at Buffalo Pass than at Illinois River. Therefore, to understand sensitivity in SNTHERM's and FASST's predictive abilities, only Buffalo Pass was chosen. This decision ensured that clear conclusions could be drawn from the results of altering the input parameters. The sensitivity analysis targeted key parameters that were thought to have a dominant effect on snow depth. The results from this sensitivity analysis are given in Figures 5.22-5.28.

Model simulations of snow depth were attempted with varying percent changes of the radiation parameters as shown in Figures 5.22-5.25. In some cases, the increased or decreased magnitude of radiation did not allow SNTHERM to complete the modeling task due to unrealistic radiation values. The predicted snow depth was plotted until the forced value became improbable. SNTHERM was not sensitive to modifications in the outgoing longwave radiation parameter or albedo as shown in Figures 5.25 and 5.28 respectively.

Incoming and outgoing shortwave radiation changes proved to have the most effect on predicted snow depth values. Even a 2% increase in incoming shortwave radiation causes SNTHERM to underpredict snow depth by an average of 0.13 m or an overall 13% absolute error rate. A 5% increase in this parameter resulted in an overall

13% underprediction of snow depth and an incomplete model run approximately half way through the melt season due to unrealistic values of incoming shortwave radiation. A 10% increase in incoming shortwave radiation simulated a 33% shallower snowpack than existed. SNTHERM calculates a shallower snowpack with increased incoming solar radiation owing to increased energy available for melt (Figure 5.22).

A 2% decrease in incoming shortwave radiation was enough to cause unrealistic values and thus an incomplete model run. However, the model was able to calculate a deeper snowpack than exists by 22% throughout most of the accumulation season. Therefore, decreasing the incoming shortwave radiation by a larger percentage caused the same error. Conversely, these forced values were not out of the models predictive window during the accumulation season. A 5% decrease resulted in a 28% increase in predicted snow depth during the accumulation season. A 10% decrease in incoming shortwave radiation resulted in a 34% overprediction of snow depth. The decrease in incoming shortwave radiation lessens the available energy to melt the snowpack and thus SNTHERM calculates a deeper snowpack (Figure 5.22).

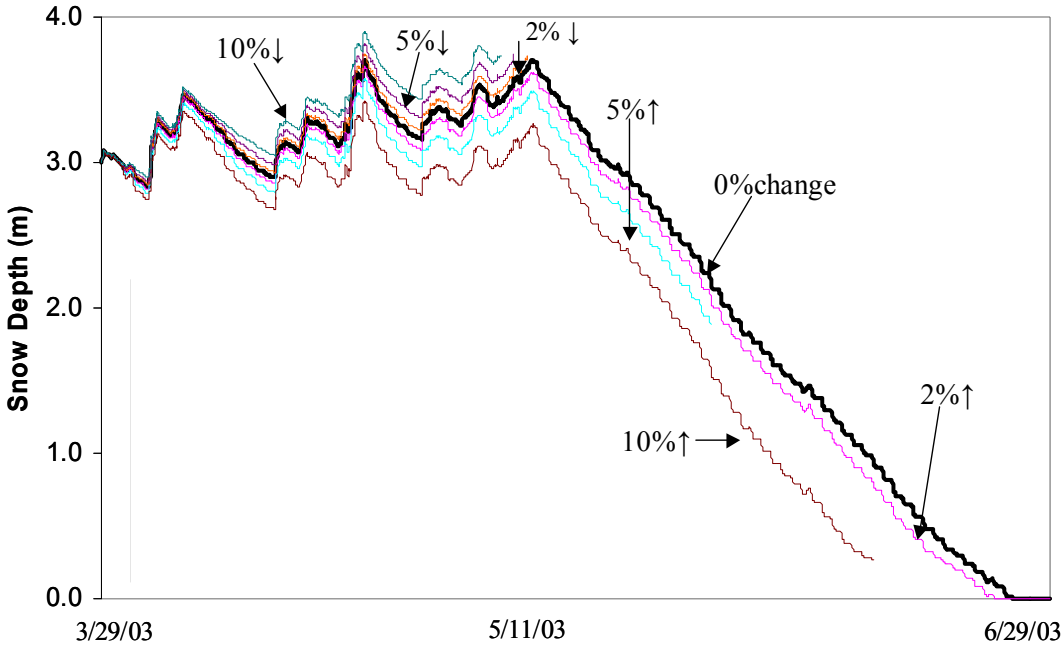

Figure 5.22. Effects of SNTHERM modeled snow depth by altering incoming shorwave radiation.

A 2% increase in outgoing shortwave radiation results in a 21% increase in predicted snow depth. SNTHERM only predicted the depth of snow through the accumulation season due to impractical values of forced outgoing shortwave radiation. Further increases in upwelling shortwave radiation also resulted in partial simulations. The consequence of forcing a 5% increase in outgoing shortwave radiation was a 40% overprediction of snow depth. Snow depth was overpredicted by 32% when the outgoing shortwave radiation was increased by 10%. The amount of outgoing shortwave radiation is one factor that determines the snowpack albedo. A greater magnitude of outgoing shortwave radiation returns a higher albedo value that suggests less energy has been

absorbed by the snowpack. Due to the non-linear energy balance calculation in SNTHERM, forcing a greater amount of outgoing shortwave radiation does not return a greater magnitude of snow depth (Figure 5.23).

An alteration of the outgoing shortwave radiation by a decreased percentage of 2% equates to a 12% decrease in estimated snow depth. Snow depth is underpredicted by 16% when outgoing shortwave is decreased by 5%. A 10% decrease in outgoing shortwave radiation causes SNTHERM to underpredict snow depth by an average depth of 0.19m or an absolute error rate of 19%. Shallower snowpacks develop when more shortwave radiation energy is absorbed. The model calculates a shallower snowpack due to the reduction of outgoing shortwave radiation and thus a decreased albedo (Figure 5.23).

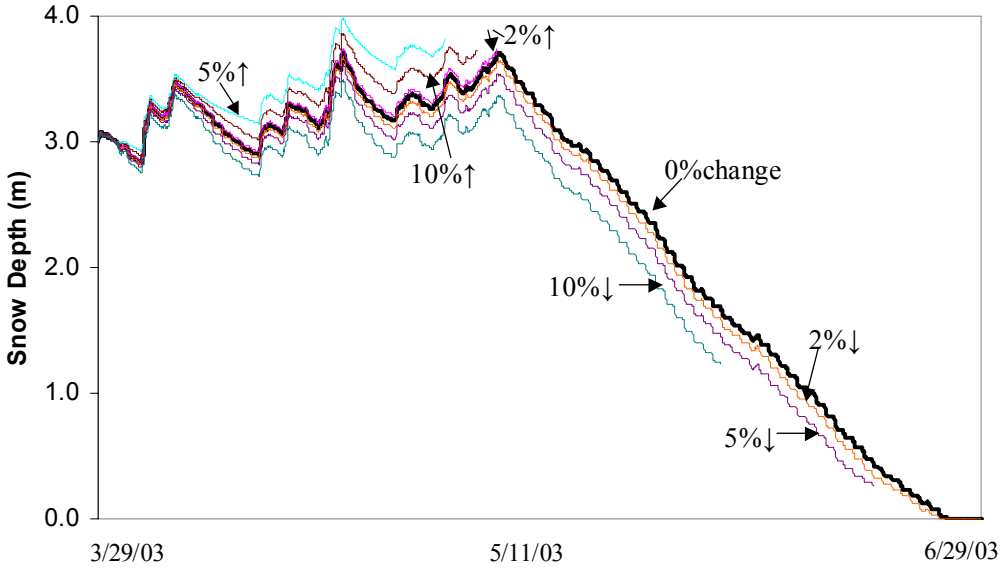

Figure 5.23. Effects of SNTHERM modeled snow depth by altering outgoing shortwave radiation.

Although SNTHERM was not sensitive to modifications in the outgoing longwave radiation, the model simulated varying seasonal snow depths based on adjustments made to the measured downwelling longwave radiation. These alterations cause a change in the overall energy balance, which determines available energy for melt of a snowpack. A 2% increase in incoming longwave radiation resulted in a 12% overprediction of snow depth. The snow depth was overpredicted by 15% when the incoming longwave radiation was increased by 5%. Increases in the incoming longwave radiation parameter did not result in shallower snow depth due to the non-linearity of the model calculations (Figures 5.24 - 5.25).

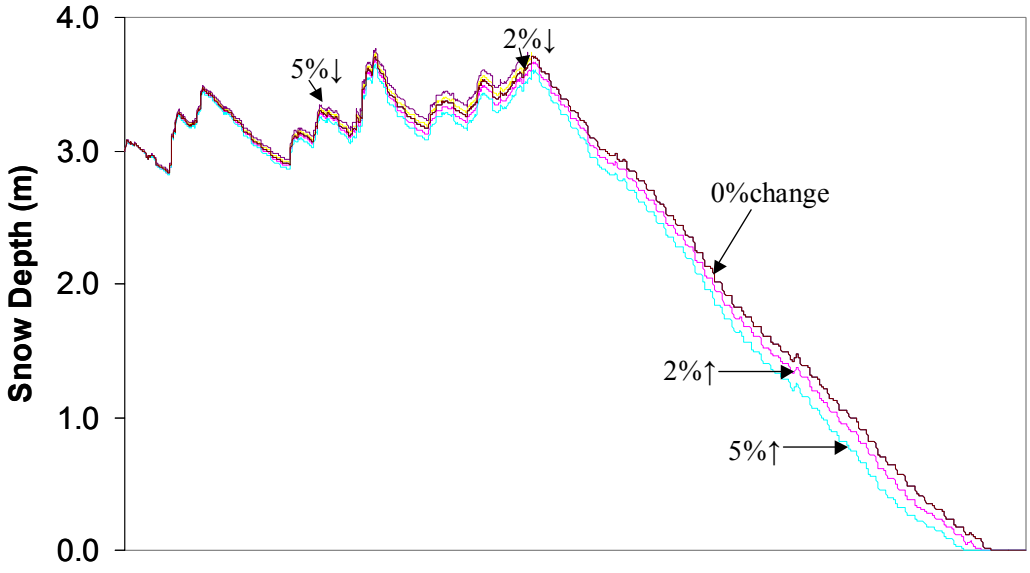

Figure 5.24. Effects of SNTHERM modeled snow depth by altering incoming longwave radiation.

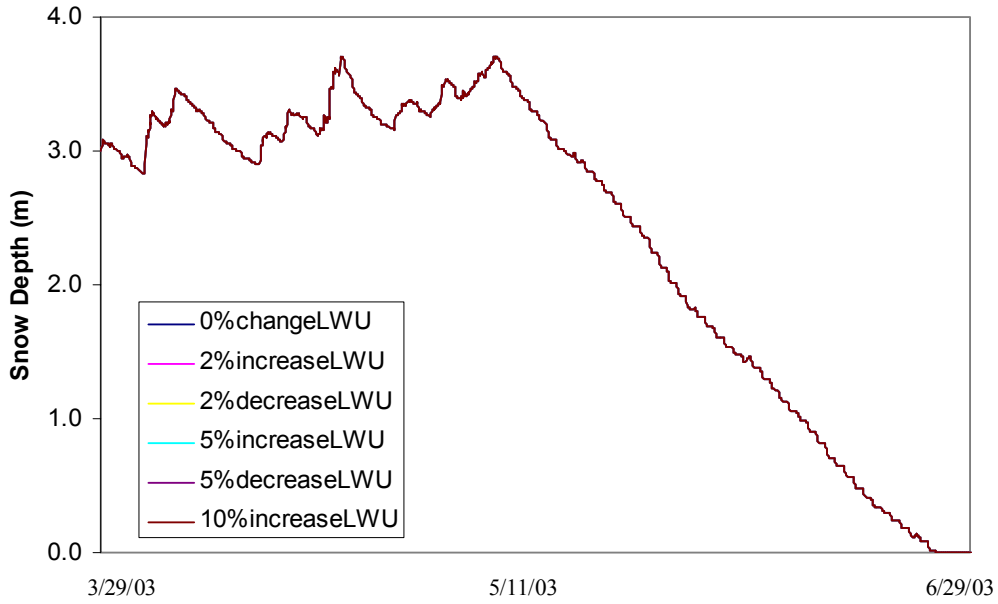

Figure 5.25. Effects of SNTHERM modeled snow depth by altering outgoing longwave radiation.

A 2% decrease in incoming longwave radiation caused SNTHERM to overpredict snow depth by 20% and disallowed a snow depth prediction further than the accumulation season due to unrealistic incoming longwave radiation values. Any other decreases in this variable also caused incomplete simulations. An applied 5% decrease in incoming longwave radiation caused a 23% deeper snowpack simulation through the accumulation period (Figure 5.25).

The new snow density was decreased from 100kg/m^3 to 80kg/m^3. The snow depth prediction resulted in an incomplete model run. By decreasing the new snow density, the model was unable to calculate snow depth throughout the chosen modeling period beyond the accumulation season. The precipitation estimation method used a new snow density of 10%, which would not justify using the lower, constant new snow

density of 80kg/m^3 for the model calculations. The model predicted a deeper snowpack by 21% with the lower new snow density value than when using the new snow density of 100kg/m^3 (Figure 5.26).

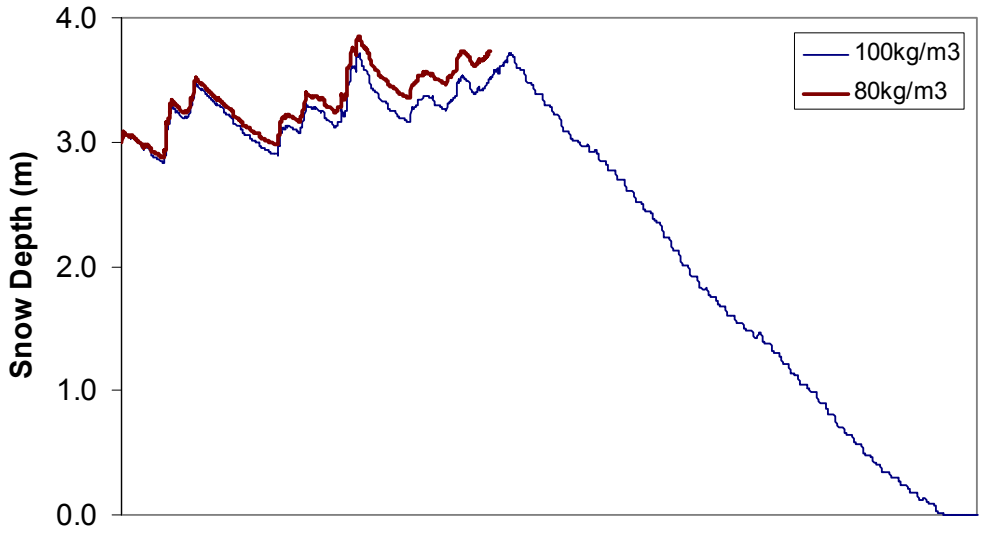

Figure 5.26. Effects of SNTHERM modeled snow depth by altering new snow density.

The albedo of the snowpack was changed to a constant value of 0.7, then 0.5 instead of allowing SNTHERM to calculate the value based on the given meteorological data. SNTHERM calculates the albedo by a method described by Marks 1988. The higher albedo value was chosen to distinguish the model response of a crude estimate of an average snowpack albedo and a lower value representative of a decaying snowpack. The results show that SNTHERM was not sensitive to changes in the constant albedo values from the model estimations of albedo when predicting snow depth due to the non-linearity of the computations (Figure 5.27).

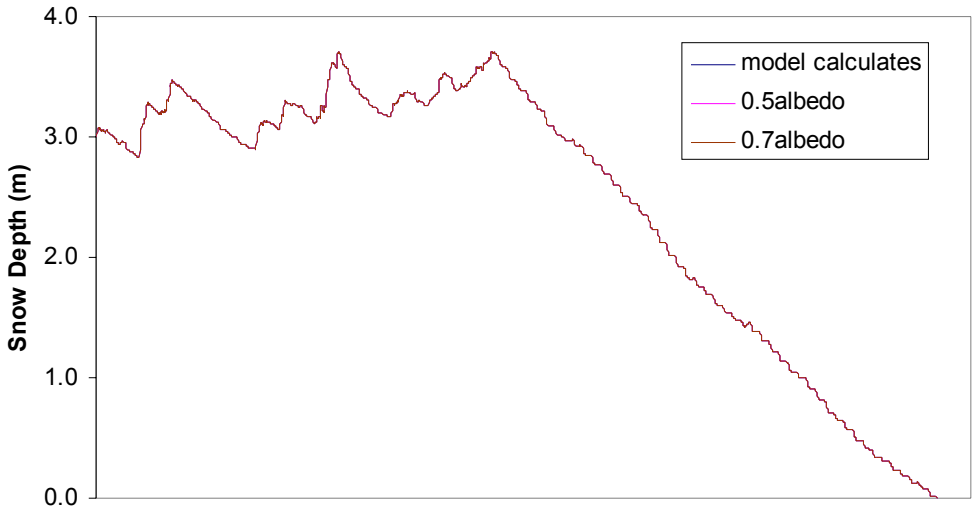

Figure 5.27. Effects of SNTHERM modeled snow depth by altering albedo.

Five degrees were added to the continuous air temperature data in order to view the new predictions of snow depth by SNTHERM. The model did not complete the snow depth prediction throughout the requested season. This circumstance occurred because the increased air temperature did not coincide with the precipitation type of snow. The model did predict a 30% increase in snow depth with an increased air temperature by 5 degrees during the accumulation period. The energy balance approximation in SNTHERM is non-linear, which causes unrealistic snow depth values when the air temperature is increased by five degrees (Figure 5.28).

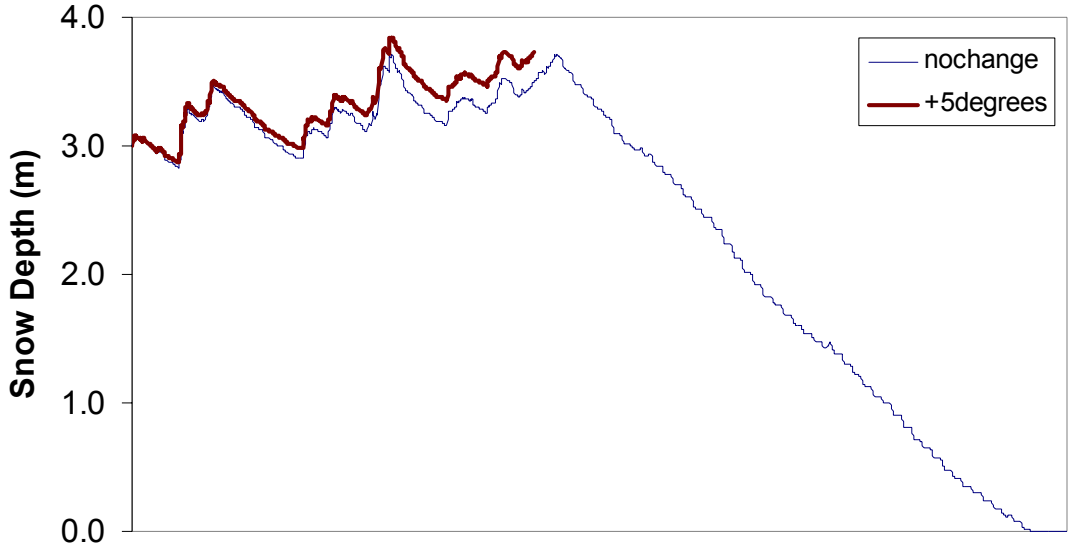

Figure 5.28. Effects of SNTHERM modeled snow depth by altering air temperature.

5.4.2. FASST

The results from the sensitivity analysis performed using FASST at the Buffalo Pass site are shown in Figures 5.29-5.32. FASST snow depth prediction was slightly sensitive to the volume of soil moisture. Alterations of the meteorological parameters such as shortwave and longwave radiation values did not affect the soil moisture predictions. This insensitivity occurred because the soil was unexposed to the elements during complete snow cover.

However, FASST soil moisture predictions were sensitive to soil type, soil layers and the presence and varying thickness of soil surface ice lenses. These sensitivities were to be expected since the soil types and layers have unique soil properties such as saturated hydraulic conductivity and bulk density. Unique soil properties or the frozen condition of the soil effect the movement of water within the soil matrix.

Figure 5.29 shows that FASST was slightly sensitive to altering the volume of soil moisture. The initial soil moisture was decreased by 30%, which resulted in less than a 1% underprediction of snow depth.

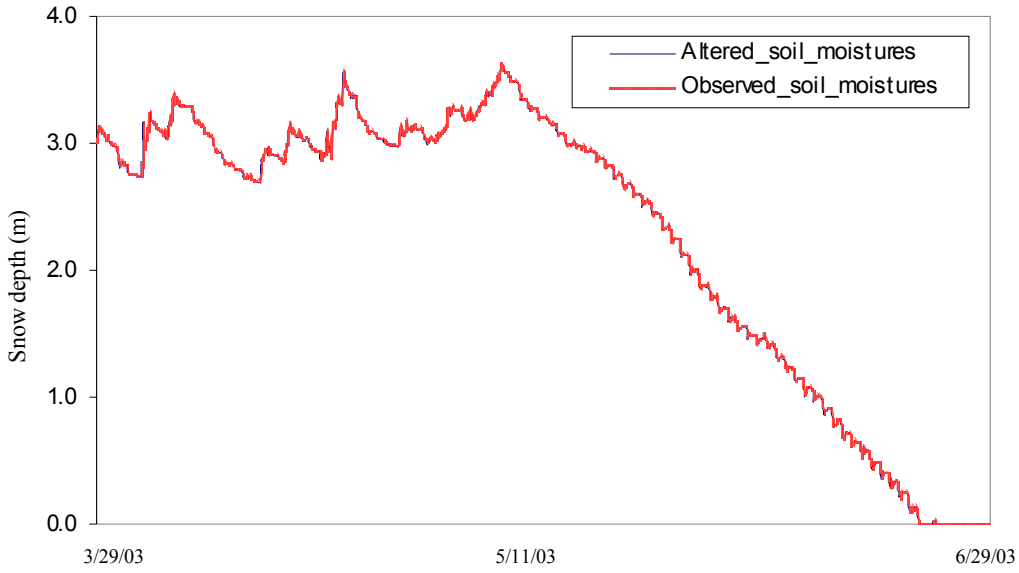

Figure 5.29. Effect on FASST snow depth by decreasing initial soil moisture values by 30%.

FASST was implemented with the SM soil type (silty sand) and compared to OH (organic silt and clay). Both simulated soil moisture results were plotted at each depth in Figure 5.30. The results show that the SM soil type caused FASST to predict less dynamic seasonal soil moisture values than the OH soil type. More variations in soil moisture were simulated using the OH soil type owing to the higher hydraulic conductivity that allows a greater flux of soil moisture in the soil matrix holding time constant. There were minimal increases or decreases in observed soil moisture. FASST did consistently show a gradual decrease in soil moisture with both soil types at the 0.50 m level on March 28 through April 10. The observations show a less dramatic, but decreasing trend during this same time frame.

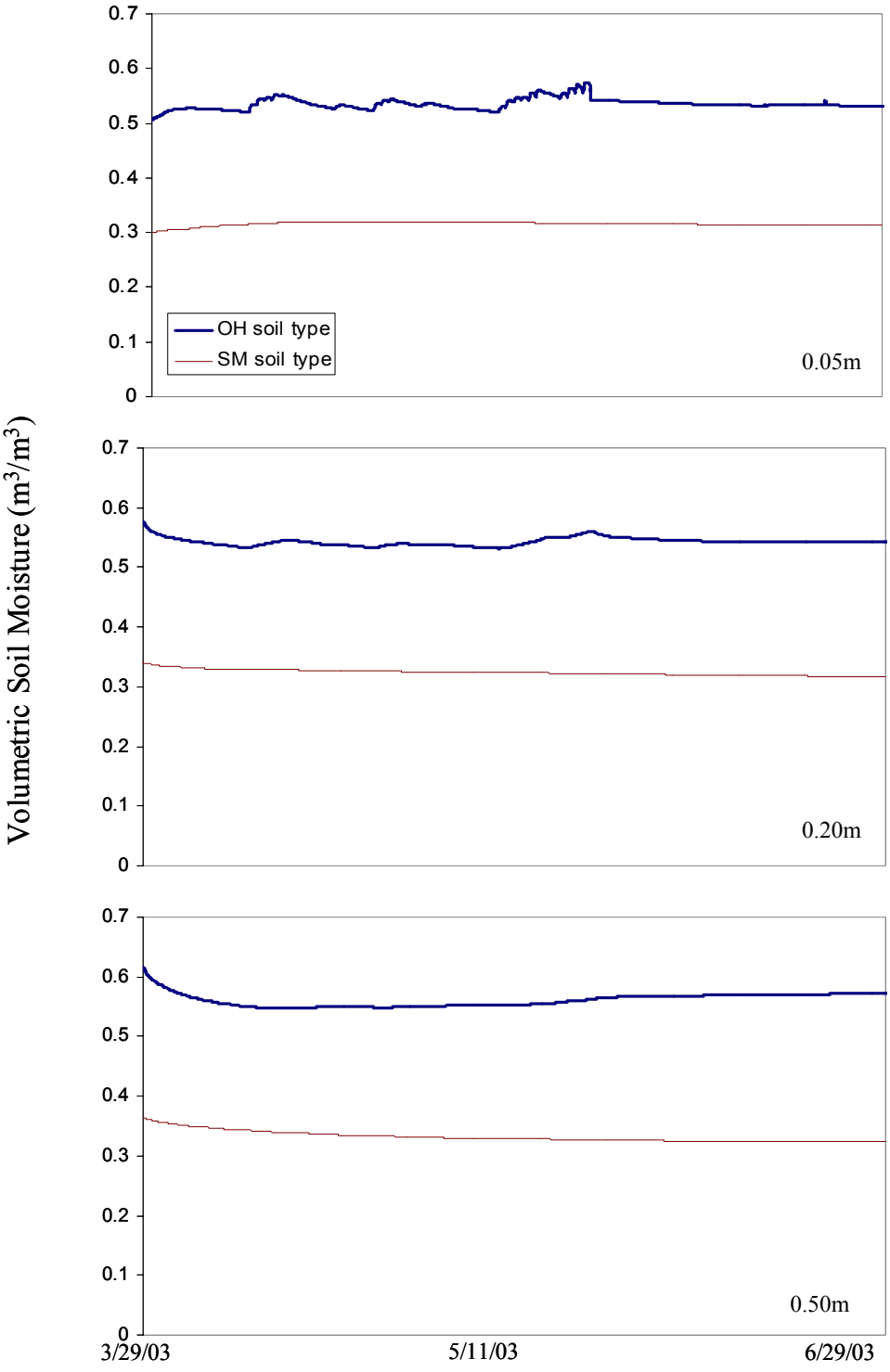

Figure 5.30. Effects of FASST predicted soil moisture by altering initial soil type.

Figure 5.31 shows the effect of dividing the soil matrix into two separate layers while applying the same soil type. The single layer was 0.50 m deep, and the double layer system was two 0.25 m layers. All other soil properties were held constant for both simulations. The soil moisture predictions were in agreement at the 0.05 m level until May 22 when the double layer simulation shows a greater decrease in soil moisture than the single layer. The single layer predicts 0.01 to 0.02 m^3/m^3 greater soil moisture values for the rest of the modeling period. The simulations at the 0.20 m level show similar results. The simulations began to diverge on April 29 and the double layer resulted in greater predicted soil moisture storage than the single layer. After May 23, the single layer results predicted more soil moisture storage. From April 15 through June 2 at the 0.50 m depth, the double layer slightly predicted more soil moisture storage than the single layer even though the shapes of the graphs were very similar.

The difference between a single and a double layer in FASST's calculations of soil moisture is due to the initial conditions that the model utilizes for the simulations. The single layer has one set of calculations to make, while the double layer system has two. The second calculation depends on the first set of output values, therefore producing slightly different initial conditions when calculating moisture for the second layer than the initial conditions that FASST commences to calculate soil moisture in the single layer.

Figure 5.32 shows that FASST was very sensitive to the presence of soil surface ice lenses and the associated thickness. The simulation with the 0.01 m ice lens showed little variation from the observations, but the 0.05 m ice lens showed a 30% increase in soil moisture at each depth on May 23. This increase in soil moisture occurred during the

snowmelt period. The predicted increase could be due to infiltration of ponded meltwater following the melt of the thicker ice lens.

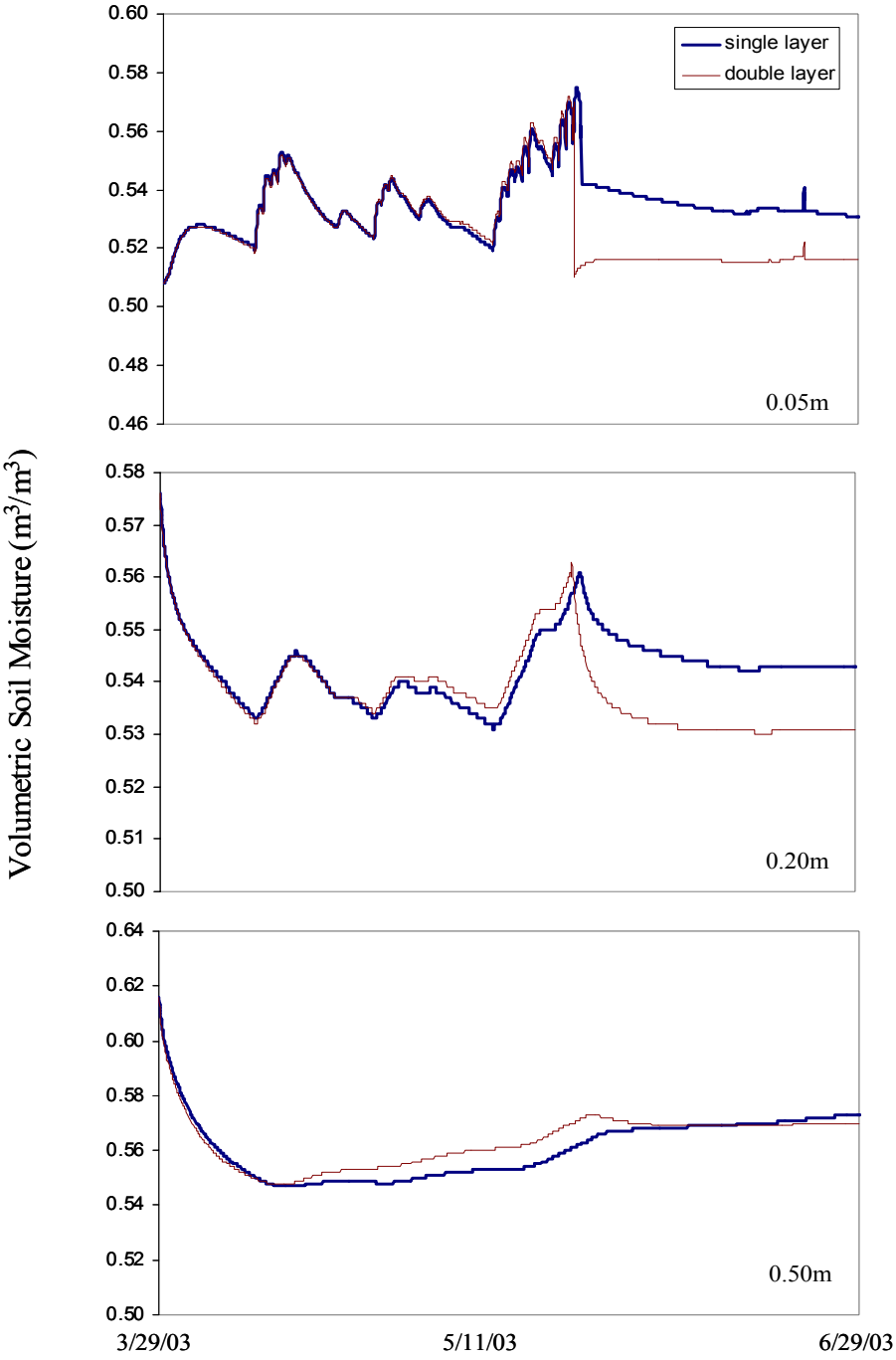

Figure 5.31. Effects of FASST predicted soil moisture by altering soil layer structure.

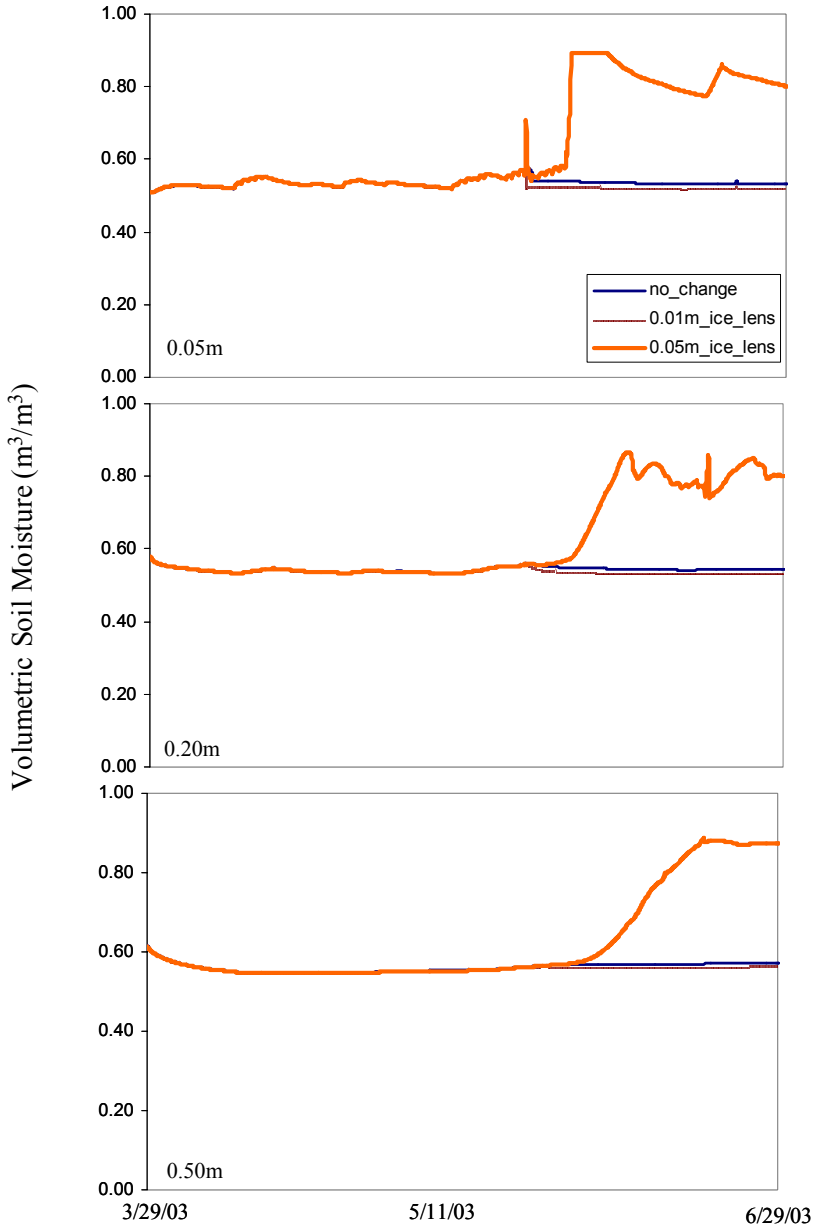

Figure 5.32. Effects of FASST predicted soil moisture by altering presence and thickness of soil surface ice lens.

CHAPTER 6. DISCUSSION

6.1. SNOW DEPTH

6.1.1. Buffalo Pass

6.1.1a. SNTHERM

The model overpredicted the snow depth during period 1 and the first five days of the melt season at the Buffalo Pass site. This overprediction made by SNTHERM was due to the snow accumulation or frost development on the incoming shortwave radiation sensor. Table 6.1 and Figure 6.1a-b show the low air temperatures and the low snow/ground temperatures as well as high relative humidity values, all of which are favorable conditions for hoar frost development. The solar angle during the accumulation season at this site and the snow or frost on the radiation measuring device can lead to under-estimation of incoming solar radiation. This under measured data can prompt the model to adjust the energy balance such that less energy is added to the snowpack and consequently predict a deeper snowpack than exists. Melloh et al. 2004 have researched snow-covered radiation sensors more in depth and show that snow development can be a problem with snow-melt modeling.

Table 6.1. Favorable conditions for hoar frost development at Buffalo Pass. Period 1 had higher humidity values and lower air temperatures than period 2.

Average Meteorological Conditions Favorable for Hoar Frost Development			
Season		Air Temperature (^{o}C)	Relative Humidity (%)
Period	1	-2	73
Period	2	7	59

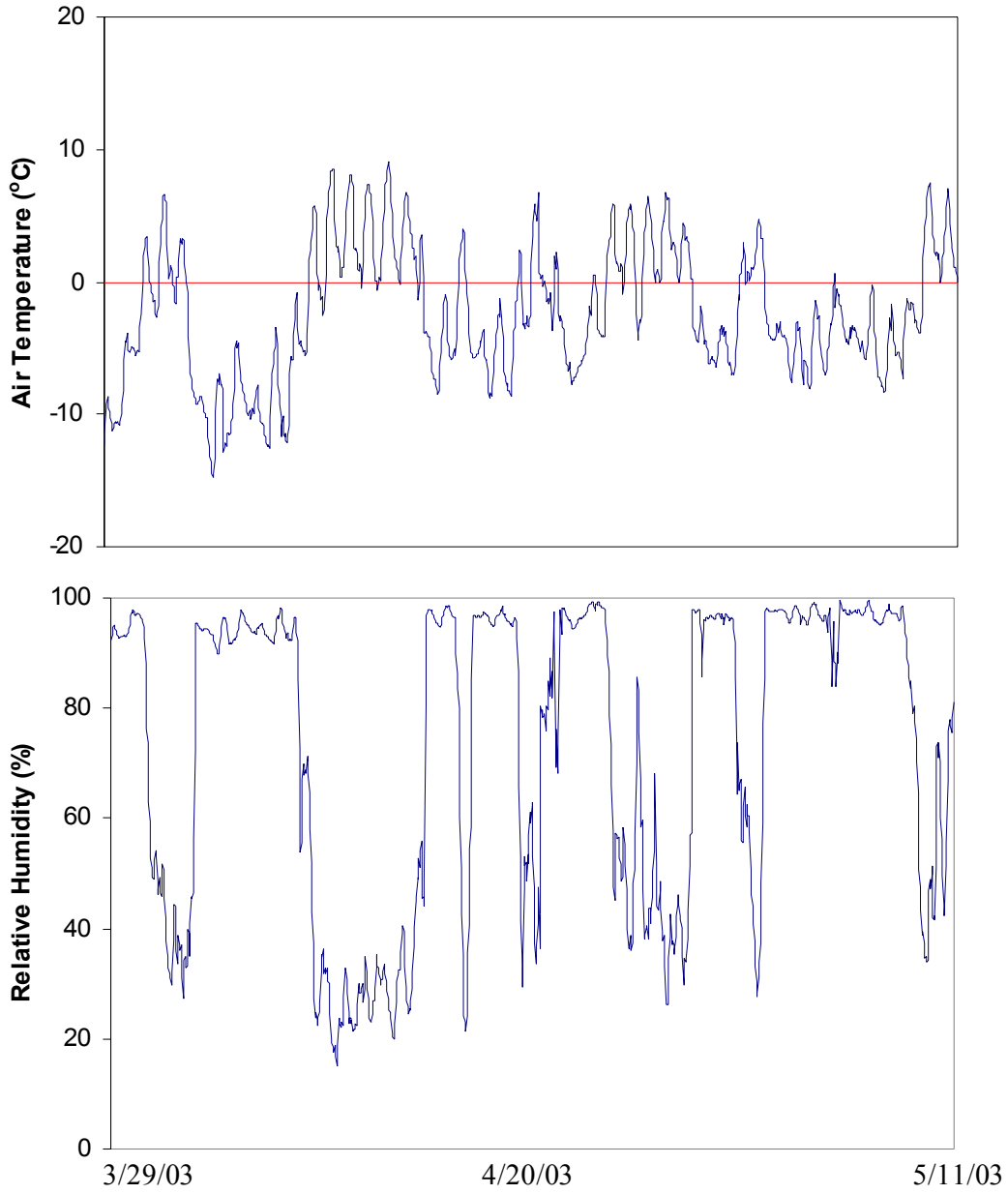

Figure 6.1 a - b. Favorable meteorological conditions for frost development on sensors. Low air temperatures (a) combined with high relative humidity values (b).

The modeled snow depth during the melt season is in excellent agreement with the observations. Figure 5.2 shows that the model slightly underpredicted the observed snow depth during a short period within the melt season. One other possibility for the "underprediction" could be instrument error. The snow depth sensor can integrate the measurement from a larger area than is calibrated for.

Figure 6.2 illustrates that SNTHERM holds the capability to model microphysical changes in seasonal snow depth. The shape and timing of the simulations are identical to most of the minute increases and decreases in the observations throughout the accumulation season even though the predicted magnitude of snow depth is offset. During the melt season, the decrease in snow depth is non-linear as shown in Figure 5.3. The graphs have "stairs", which represent the diurnal melt-freeze cycles. The negative slope would represent the melt, while the zero slopes would represent the freeze period.

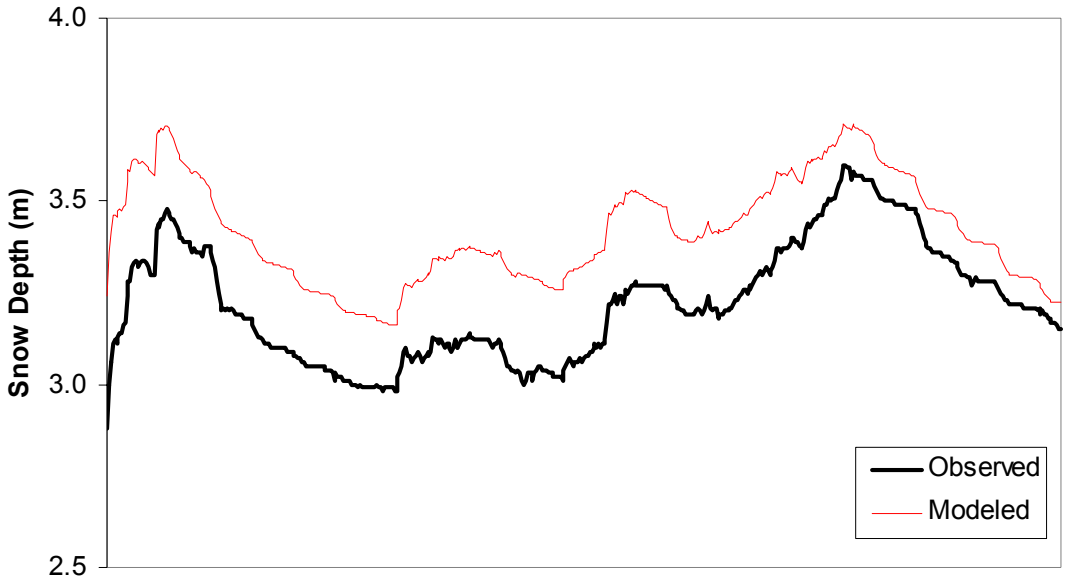

Figure 6.2. SNTHERM predicts microphysics of snow depth at Buffalo Pass.

The predicted snow cover depletion date was within an accurate time frame as the observations. The physically based nature of SNTHERM's energy balance approximations allows for an accurate estimate of snow cover depletion timing.

6.1.1b. FASST

FASST estimated snow depth evolution with excellent accuracy. FASST's less complex internal configuration resulted in better snow depth approximations than SNTHERM. FASST calculates snow depth by presuming a single layer of snow with constant snowpack properties. SNTHERM permits infinite snowpack layer structure along with associated densities, temperatures and snow grain sizes. Andersson et al. (1992) explained that as model complexity increases initially, the accuracy of the results increases, but as the model complexity increases beyond a threshold, model performance accuracy decreases considerably.

FASST predicted snow cover depletion dates at Buffalo Pass excellent. FASST used the continuous snow depth observations, which allowed the model to predict the snow cover depletion date closer to the observed date than SNTHERM.

Another reason for the remarkable snow depth results from FASST was that the model used the observed time series snow depth to calculate snow depth. The model replaces any simulated snow depth inconsistency between single time steps with the observed snow depth value at the following time step.

The new simulations without the usage of the continuous snow depth observations produced inaccurate snow depth magnitudes and the snow cover depletion date. The timing of snow depth observation changes was accurately represented Figure 5.8. The

model calculates snow depth using constant snowpack properties, assumes a single snowpack layer and is not as physically based as SNTHERM. The model inaccurately estimated snow depth magnitude most likely because the properties of the snowpack assumed were not representative of the observed snowpack.

6.1.2. Illinois River

6.1.2a. SNTHERM

There are several reasons as to why SNTHERM overpredicted snow depth at Illinois River. One possibility is that the model does not account for blowing snow. Recall that the shallow and temporal variability of snow cover and the highly dynamic meteorological conditions create an extremely difficult modeling environment. Figure 5 shows that during period 1 the wind speed rapidly increased from 0.5 m/s to 8m/s on March 1. In this case, the model would predict snow accumulation instead of calculating loss of snow due to wind scour.

One other source of incorrect snow depth predictions could be due to the precipitation estimates that are based on accumulations of snow depth using assumed water content. A calculated water content of precipitation that is higher than the true value, leads to a dense snowpack and thus the model would predict a shallower snowpack than exists. At other times during the modeling season, the new snow density could be too high, which would result in an underprediction of snow depth.

The snow cover depletion date was forecasted in an accurate time frame comparable to the observations. SNTHERM is physically based such that the model not only predicted snow depth reasonable, considering the highly dynamic observed

meteorological patterns, but also was able to calculate the depletion date of an extremely variable and shallow snow cover within one day of the observations.

6.1.2b. FASST

FASST predicted the snow depth more accurately than SNTHERM due partly to the level of model complexity. FASST assumes a single layer of snow and constant snowpack properties, while SNTHERM allows numerous layers along with various layer densities, temperatures and snow grain sizes. Andersson et al. (1992) explained that initially with increase in model complexity, the performance accuracy increases, but as the model complexity increases further, model performance accuracy drastically decreases.

The timing of the snow cover depletion was also accurately replicated. FASST used the time series snow depth observations that assisted in forecasting the snow cover depletion date. FASST is much computationally simpler than SNTHERM, but was able to calculate the snow cover depletion date of a variable and shallow snow cover.

Another reason for the excellent performance rate of FASST was due to the usage of the continuous snow depth observations in the model calculations of snow depth. The model updates any simulated snow depth discrepancy between the previous time step and the new time step with the observed snow depth value at the new time step.

Figure 5.14 shows that the estimated snow depth derived without using the continuous snow depth observations was problematic for FASST. The simulations overpredicted the magnitude of snow depth by an overall 4.5%, but the timing of snow depth changes was accurately replicated. The snow depth magnitude was inaccurate, but

the prediction did not prove as problematic for Illinois River than as for Buffalo Pass. The single layer assumption and constant snowpack properties used by FASST were reasonable estimates for snow depth magnitude and timing predictions considering the highly spatially and temporally variable shallow nature of the snow cover at Illinois River.

6.2. SOIL MOISTURE

6.2.1. Buffalo Pass

The model performance of FASST was accurate overall. FASST predicted the quantity of soil moisture and the timing of soil moisture changes with error rates less than 10% as listed in Table 5.6. The model did predict more peaks and valleys in the soil moisture than the observed. For example, Figure 5.16a - b shows that in the 0.05 m and 0.20 m depth, the dynamics in the modeled soil moisture plot resembles the snow depth variations.

The user has the capability of implementing FASST with detailed soil data. Many combinations of various soil types, layers, and hydraulic properties were attempted. In order to make fewer assumptions about the soil data, the default soil types and the associated soil properties that more closely represented the soil type collected from soil surveys were used.

The most obvious problem could be with the lack of soil data available. The only soil information obtainable from a source besides FASST defaults was the soil type that was collected from a soil survey measurement. The model default soil properties that were associated with the measured soil type of OH (highly organic sand, silt and clay

fractions) were used in the simulations. While this soil type is an appropriate choice for the soil surface at this site, the underlying layers of the soil are unknown. The soil matrix may contain more inorganic matter than is accounted for in the simulations.

Another possible problem with the lack of soil data is that the observed soil may be saturated upon the snow cover depletion date. The OH soil type allows a greater soil moisture capacity than the initial measured soil moisture. If the soil were saturated at snowmelt, the meltwater would not infiltrate. The saturated condition of the soil could explain why the observations do not show an increase of soil moisture storage after the snowmelt season at this site, but the model allows increases of soil moisture. The observations on Figure 5.16a show an increase in soil moisture at the near surface layer during the snow accumulation season. The observations show that the soil moisture decreases at all levels following snowmelt. Without the presence of snow cover for soil insulation, evaporation can commence.

FASST does not handle lateral flow movement in the soil. The model exclusively forecasts soil moisture transport due to gravity. If water only moved vertically in the soil matrix, results of infiltrating water into the column could demonstrate a larger increase owing to a smaller volume to fill.

An explanation for FASST's underpredictions of the soil moisture values at all depths could be that the model allows more drainage of the soil moisture than is actually occurring. The model assumes the minimum hydraulic conductivity of the user specified soil type for draining. Since the layered soil information is not available, it is uncertain as to whether or not the model excessively drained the stored soil moisture.

Lastly, the volumetric soil moisture observations are questionable. The soil moisture probes were not given time to equilibrate before trusting the measurements.

6.2.2. Illinois River

FASST would not produce results beginning at the same time step as the SNTHERM model was initiated. The model developer included a code that would not allow the model to run to completion if there were a 20 degrees or greater temperature fluctuation between two time steps. The snowpack initial surface temperature was input as 0^{o}C. The model yielded an error message when the air temperature dropped below -20^{o}C, which occurred on March 1.

There are numerous possibilities as to why the model did not predict all of the peaks and valleys of the soil moisture or the magnitude of the soil moisture changes. One possible reason is that the soil property measurements and data did not sufficiently represent the soil. The soil type was input as a single layer soil system into FASST. The actual layered soil type at Illinois River is unknown.

The placement of the soil moisture probes could be problematic for FASST. The probes are not located directly under the snow depth sensor. In conjunction with soil moisture being highly spatially variable, the presence of snow is extremely inconsistent from space to space at Illinois River. This variable situation along with the differing locations of the instrumentation creates an extremely complex soil moisture modeling environment.

The other possible problem is that the possible soil moisture inputs were so minimal that FASST did not predict an increase in soil moisture. For example, the snow

depth is less than 0.30 m for the chosen modeling period. A crude estimate of SWE based on the snow depth at this site is 0.03 m. This small amount of water is difficult to predict since the status of snow cover directly above the soil moisture probes was unknown.

Another complication in comparing the observations to the modeled soil moisture at this site was that the actual ice content within the soil was not calculated from the soil moisture probes. Figure 6.3 shows two periods where the snow/ground temperature was at or below 10^{o}C, while the 0.05 m soil temperature was measured at 0^{o}C. During these two periods, the soil moisture observations showed a dramatic change. The soil probe manual instructed to average the point before and the point after the dramatic change in soil moisture to obtain soil liquid moisture content without the ice fraction. A separate software package is included to calculate the ice content but was not used for this research. The results from FASST include soil moisture (ice content + liquid water content = total soil moisture).

Yamaguchi et. al (2002) explain that most models that estimate soil moisture that incorporate meteorological data and that apply heat and water fluxes into the soil have difficulties in calculating the quantity of soil moisture due to the emphasis on predicting evaporative fluxes.

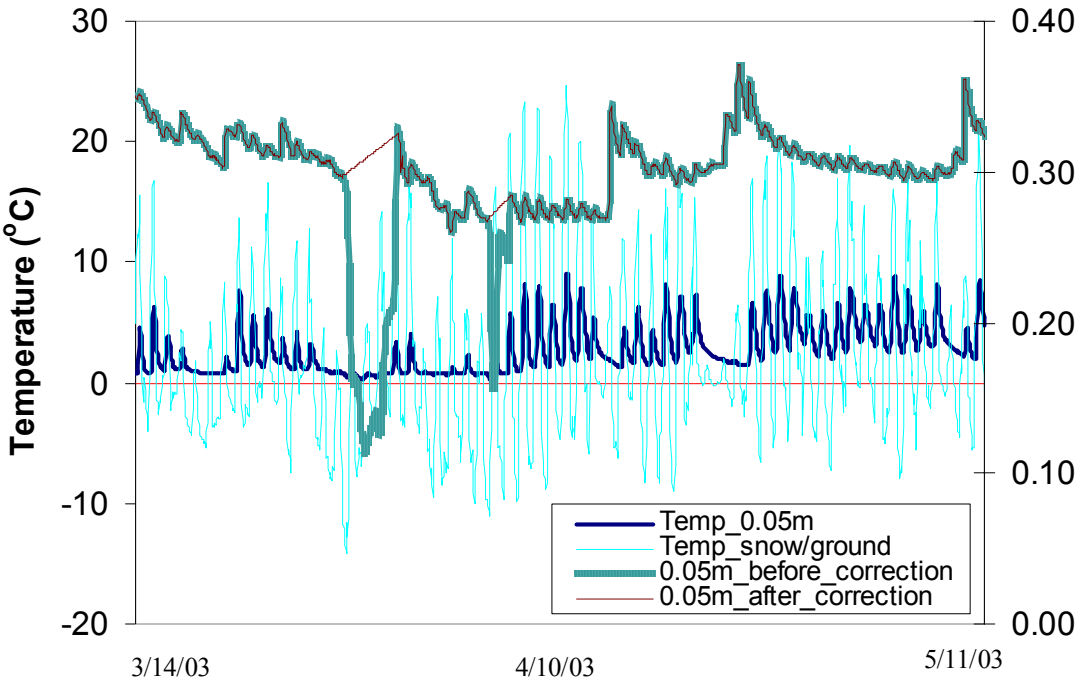

Figure 6.3. Temperature of soil at 0.05 m below the soil surface, temperature at the snow/ground interface, raw soil moisture data at 0.05 m below the soil surface and corrected soil moisture at 0.05 m below the soil surface at Illinois River. The correction shows measured liquid water content and does not include any frozen soil moisture. Note that during the 'dips' in the non-corrected soil moisture correspond with snow/ground temperatures that drop to and and below –10°C and the 0.05 m soil temperature falls to the freezing point. The Steven Vitel probes have a separate software package to calculate the ice content during these 'dips'.

6.3. PROS AND CONS OF SNTHERM AND FASST

6.3.1. SNOW DEPTH

6.3.1a. SNTHERM Pros and Cons

The advantage of physically based models such as SNTHERM is the representative nature of the observations. SNTHERM allows the user to input snowpack initial conditions that use little to no assumptions about the data. The model allows infinite snowpack layers that represent the observed stratigraphy with associated layer snow temperature, snow density and snow grain size.

Another plus to using SNTHERM for predictions snow depth evolution and snow cover depletion is that the model does not require any subsequent snowpack data for the entire modeling period beyond the detailed initial conditions.

A disadvantage to SNTHERM is that the model is computationally complex. For every initial condition, the model uses several numerical approximations to update the data for every time step. The excessive computations can lead to modeling errors such as explained in the sensitivity analysis of this paper. For instance, theoretically as downwelling longwave radiation magnitude is increased, snow depth should decrease due to added energy onto the snowpack. However, Figure 5.24 shows that SNTHERM does not predict such decreases in snow depth given increased magnitude of the incoming longwave radiation due to the non-linearity of the calculations made by SNTHERM.

Other shortcomings of SNTHERM include the lack of blowing snow and vegetation routines. Figure 4.2a,d at Illinois River shows an overprediction of snow depth was calculated that could have been accounted for if a blowing snow component

was built into SNTHERM. A third field site was initially chosen to explore the models predictive abilities, but the SNTHERM results were unacceptable due to the models inability to account for vegetation. The meteorological parameters were measured within a pine forest canopy, but the model assumed the data was collected from an open environment. The energy balance calculations made by SNTHERM described a snowpack unsheltered by trees, which resulted in an extreme underprediction of observed snow depth (Figure 6.4).

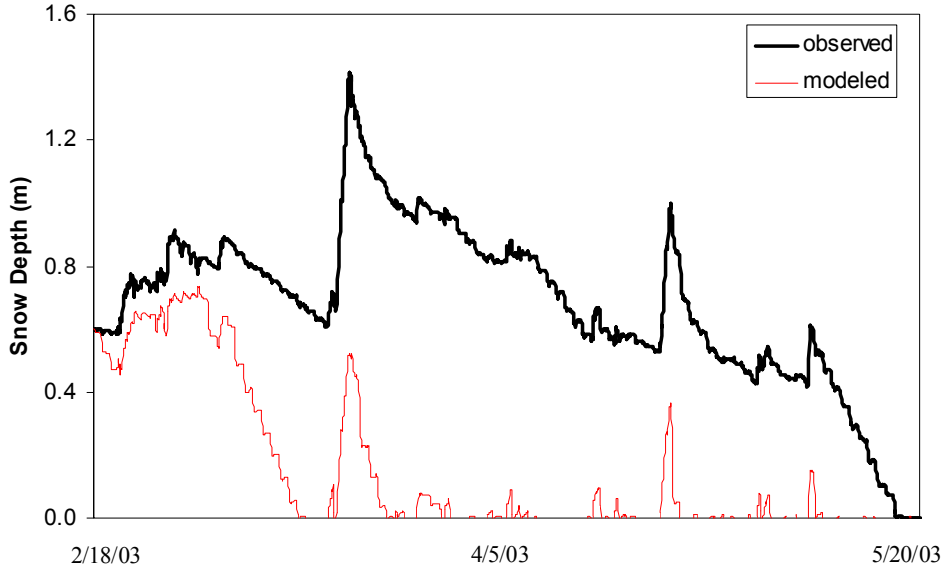

Figure 6.4. St. Louis Creek, Colorado. SNTHERM underpredicted snow depth based on meteorological measurements made within a forest canopy. The model assumed the measurements were made in an open environment.

6.3.1b. FASST Pros and Cons

An advantage to using FASST to predict snow depth is the simple computations involved. FASST assumes constant snowpack properties for the initial conditions so that the only initial requirement is snow depth. If initial snowpack data such as snow grain size or snow density is not available the model is still able to calculate a snow depth.

Conversely, if continuous snow depth measurements are available, FASST will update any modeled discrepancy with the observation at the new time step. This modeled snow depth will be a very accurate estimate of snow depth. The results from FASST that used the continuous snow depth measurements (Figure 5.5 and Figure 5.11) show that the model performed very accurately. Without using the time series snow depth data, the model predicted snow depth more accurately at the shallow snowpack site, Illinois River (Figure 5.14) than Buffalo Pass that is characteristic of a deep snowpack (Figure 5.8). Accurate estimates of temporally variable and shallow snowpacks are challenging for models, but FASST has expressed the ability for predicting the evolution of the Illinois River shallow and inconsistent snowpack.

A disadvantage of using FASST to predict deep snowpacks when observations of snow depth are not accessible is that the model could yield results that extremely overpredict the magnitude of snow depth, which was the case at Buffalo Pass (Figure 5.8). The constant snowpack properties used for the snow depth predictions may not be physically representative of the true initial snowpack conditions.

FASST lacks a vegetation routine. Without accounting for vegetation, models assume the energy balance is that of an open environment, which complicates obtaining

an accurate snow depth estimate. The vegetation computational procedure is currently being added to the model.

6.3.2 Soil Moisture

6.3.2a. FASST Pros and Cons

The advantage to soil moisture prediction in FASST is due to the straightforward internal estimations. The one-dimensional nature of the model requires only a few initial soil conditions such as the initial soil surface ice condition. Default soil types and properties can be used in the soil moisture calculations if soil data is unavailable. Figure x and x show that the model was capable of calculating accurate soil moisture recharge and seasonal soil moisture volumes with using limited soil property data.

However, a lateral flow component to the soil moisture calculations could lead to more accurate estimations of soil moisture. The model only moves water due to gravity flow, but adding a physically based capillary movement to the computations may increase the soil water storage and moisture recharge estimations made by FASST.

CHAPTER 7. CONCLUSIONS

SNTHERM accurately modeled snow cover depletion at Buffalo Pass and Illinois River. The model predicted the timing of accumulation and melt and the magnitude of snowpack depth throughout the entire modeling period correctly. The highly spatially variable pattern of snow cover and variable meteorological conditions at Illinois River proved to be challenging for SNTHERM in predicting the magnitude of snow depth on a relative scale, but the overall fit was excellent. Nonetheless, the snow cover depletion date occurred only two days after the observations at Buffalo Pass and one day prior to the observations at Illinois River.

The SNTHERM and FASST model performance statistics prove that FASST predicted the timing of accumulation and melt and the snow depth magnitude at both sites more accurately than SNTHERM, when continuous snow depth observations were used for FASST. SNTHERM and FASST both predicted the snow cover depletion date one day earlier than the observations at Illinois River. FASST forecasted the snow cover depletion date on the exact day that the observations reveal at Buffalo Pass, while SNTHERM predicted the complete snow melt date two days later than the observations. FASST performed more accurately overall due to the lower complexity of the snow depth calculations than SNTHERM even though both models produced excellent snow depth evolution results. Conversely, FASST produced inaccurate snow depth results when the continuous snow depth observations were not supplied.

The soil moisture results from FASST and model performance statistics at Buffalo Pass indicate that the model accurately predicted the quantity of seasonal soil moisture.

The estimated soil moisture values were within $0.10 m^3/m^3$ of the observed soil moistures. The model overpredicted the magnitude of soil moisture at Illinois River. The simulations did not precisely replicate the observed increases, decreases and soil moisture recharge at both sites at 0.20 m and 0.50 m. Measured values of hydraulic soil parameters and soil layer data would enable FASST to calculate the evolution of soil moisture and soil moisture recharge more accurately by using observed soil parameters instead of default soil values. A lateral flow component in the model configuration would assist in more accurate soil moisture recharge results because the soil matrix would not be limited to one dimensional flow and storage.

SNTHERM and FASST correctly modeled snow cover depletion and soil moisture recharge at Buffalo Pass and Illinois River overall. The graphical representations of the snow depth and soil moisture simulations and the associated model performance statistics reveal that SNTHERM and FASST predict the respective parameters favorably. Both SNTHERM and FASST are useful models that can assist in hydrologic applications.

8. REFERENCES

Andersson L. 1992. Improvements of runoff models - Which way to go? *Nordic Hydrology* **23**: 315-332.

Asch Th, Dijck S, Hendricks M. 2001. The role of overland flow and subsurface flow on the spatial distribution of soil moisture in the topsoil. *Hydrological Processes* **15**: 2325-2340.

Baral D, Gupta R. 1997. Integration of satellite sensor data with DEM for the study of snow cover distribution and depletion pattern. *International Journal of Remote Sensing* **18**(18): 3889-3894.

Cherkauer K, Bowling L, Lettenmaier D. 2003. Variable infiltration capacity cold land process model updates. *Global Planet Change* **38**(1-2): 151-159.

Cline D, Elder K, Davis R, Hardy J, Liston G, Imel D, Yueh S, Gasiewski A, Koh G, Armstrong R, Parsons M. 2003. Overview of the NASA Cold Land Processes Field Experimental (CLPX - 2002). Microwave Remote Sensing of the Atmosphere and Environment III , Kummerow C, JingShang J, Uratuka, Editors, Proceedings of SPIE; **4894**: 361 - 372

Dunne T, Leopold L. 1978. *Water in Environmental Planning.* W.H. Freeman and Company: New York; 163-189 pp.

Faria D, Pomeroy J, Essery R. 2000. Effect of covariance between ablation and snow water equivalent on depletion of snow-covered area in a forest. *Hydrological Processes* **14**: 2683-2695.

Flerchinger G, Saxton K. 1987. *Simultaneous Heat and Water Model of a freezing snow-residue-soil system*. ASAE winter meeting 87-2567: 1-21.

Frankenstein, S. 2003. *Fast All season Soil STrength (FASST).* PhD draft. Unpublished manuscript: 1-83.

Granger R., Chanasyk D, Male D, Norum D. 1977. Thermal regime of a prairie snow cover. *Soil Society of American Journal* **41**: 839-842.

Gray D, Toth B, Litong Z, Pomeroy J, Granger R. 2001. Estimating areal snowmelt infiltration into frozen soils. *Hydrological Processes* **15**: 3095-3111.

Groffman P, Hardy J, Nolan S, Fitzhugh R, Driscoll C, Fahey T. 1999. Snow depth, soil frost and nutrient loss in a northern hardwood forest. *Hydrological Processes* **13**: 2275-2286.

Gustaffson D, Stahli M, Jansson P. 2001. The surface energy balance of a snow cover: comparing measurements to two different simulation models. *Theoretical and Applied Climatology* **70**: 81-96.

Hardy J, Davis R, Jordan R, Ni W, Woodcock C. 1998. Snow ablation modeling in a mature aspen stand of the boreal forest. *Hydrological Processes* **12**: 1763-1778.

Harms T, Chanasyk D. 1998. Variability of snowmelt runoff and soil moisture recharge. *Nordic Hydrology* **29** (98): 179-198.

Hinzman L, Kane D. 1991. Snow hydrology of a headwater arctic basin 2. Conceptual Analysis and Computer Modeling. *Water Resources Research* **27**(6): 1111-1121.

Jin J, Xiaogang G, Sorooshian S, Zong-Liang Y, Bales R, Dickinson R, Shu-Fen S, Guo-Xiong W. 1999. One-dimensional snow water and energy balance model for vegetated surfaces. *Hydrological Processes* **13**: 2467 – 2482.

Jordan R. 1991. *A one-dimensional temperature model for a snow cover.* Technical Documentation for SNTHERM.89; USA Cold Regions Research and Engineering Laboratory, Special Report 657.

Julander R, Cleary S. 2001. Soil moisture data collection and water supply forecasting. *Proceedings of the 60th Annual Meeting of the Western Snow Conference*; Sun Valley Idaho: 77-84.

Levine E, Knox R. 1997. Modeling soil temperature and snow dynamics in northern forests. *Journal of Geophysical Research* **102** (D24): 29407 - 29416.

Liston G. 1999. Interrelationships among snow distribution, snowmelt, and snow cover depletion: Implications for Atmospheric, Hydrologic, and Ecologic Modeling. *Journal of Applied Meteorology* **38**: 1474-1487.

Male D, Gray D. 1981. *Handbook of Snow, Principles, Processes, Management and Use*. D.M. Gray and D. H. Male, Editors, Pergamon Press: Toronto; New York; 360-436 pp.

Marks D. 1988. *Climate, energy exchange, and snowmelt in Emerald Lake watershed, Sierra Nevada*. PhD thesis, University of California at Santa Barbara.

Marks D, Winstral A. 2001. Comparison of snow deposition, the snow cover energy balance, and snowmelt at two sites in a semiarid mountain basin. *Journal of Hydrometeorology* **2**(3): 213-227.

Marks D, Winstral A. 2002. Simulation of terrain and forest shelter effects on patterns of snow deposition, snowmelt and runoff over a semi-arid mountain catchment. *Hydrological Processes* **16**: 3605-3626.

Melloh R, Hall T, Bailey R. 2004. Radiation data corrections for snow-covered sensors: are they needed for snowmelt modeling? *Hydrological Processes* **18**: 1113-1126

Pomeroy J, Gray D, Shook K, Toth B, Essery R., Pietroniro A, Hedrstrom N. 1998. An evaluation of snow accumulation and ablation processes for land surface modeling. *Hydrological Processes* **12**: 2339-2367.

Rowe C, Kuivinen K, Jordan R. 1995. Simulation of summer snowmelt on the Greenland ice sheet using a one-dimensional model. *Journal of Geophysical Research* **100**(D8): 16265-16273.

Seyfried M, Murdock M, Hanson C, Flerchinger G, Vactor S. 2001. Long-term soil water content database, Reynolds Creek Experimental Watershed, Idaho, United States. *Water Resources Research* **37**(11): 2847-2851.

Shook K, Gray D, Pomeroy J. 1993. Temporal variation in snow cover area during melt in prairie and alpine environments. *Nordic Hydrology* **24**: 183-198.

Willis W, Carlson C, Alessi J, 1960. Depth of freezing and spring run-off as related to fall soil-moisture level. *Canadian Journal of Soil Science* **41**: 115-123.

Yamaguchi Y, Shinoda M. 2002. Soil moisture modeling based on multiyear observations in the Sahel. *Journal of Applied Meteorology* **41**: 1140 – 1146.

APPENDIX A

Parameter Definitions

α = albedo

α_{top} = substrate surface albedo

b = ice, liquid, vapor, air

β = compressibility of water (4.4×10^{-10} Pa^{-1})

c = specific heat ($J/Kg \cdot K$)

C = condensation rate (m/s)

D = diffusion rate (m^2/s)

D_s = snow depth (m)

ρ = density (kg/m^3)

ρ_t = density of combined solid and liquid in snowpack (kg/m^3)

e = dirt, water, ice or air

E = evaporation rate (m/s)

f = fraction of precipitation that goes through freezing process

f_l = wet fraction or snowpack

g = gravity (m/s^2)

γ = bulk density of the snowpack (kg/m^3)

h = total head (m)

$h_{i,melt}$ = head from melting ice (m)

h_{pond} = head from ponding water (m)

$h_{s,melt}$ = head from melting snow (m)

H = sensible heat (W/m^2)

H_i = ice thickness per unit area (m)

I_c = convective heat flux (W/m^2)

$I_{ir\downarrow}$ = downwelling longwave radiation (W/m^2)

$I_{ir\uparrow}$ = upwelling longwave radiation (W/m^2)

I_l = latent heat flux (W/m^2)

I_s = sensible heat flux (W/m^2)

$I_{sw\downarrow}$ = downwelling solar radiation (W/m^2)

I_{top} = input energy at the surface of the snowpack (W/m^2)

j = nodal index of control volume

J = flux (convective, diffusive or combination of the two)

k = thermal diffusivity (m^2/s)

κ = thermal conductivity ($W/K \cdot m$)

K = hydraulic conductivity (m/s)

l_{fus} = latent heat of fusion (3.335×10^{-5} J/kg)

L = latent heat (J/kg)

m = from the Van Genuchten equation (1 - 1/N)

n = soil porosity

N = Van Genuchten constant related to pore size

η = viscosity ($kg/m \cdot s$)

Ω = general quantity in conservation equations

P = precipitation energy (W/m^2)

P_r = precipitation rate (mm/hr)

avg (P_s) = average load pressure in snowpack ($g \cdot sm/s^2$)

ø = soil compressibility (Pa^{-1})

q = mass flux ($kg/m^2 \cdot s$)

Q = nodal energy (J/m^3)

$R_{\downarrow}$ = incoming infrared radiation (W/m^2)

$R_{\uparrow}$ = outgoing infrared radiation (W/m^2)

S_s = soil storativity

S_w = net solar radiation (W/m^2)

S = source density (kg/m^3)

t = time (sec)

T = temperature (K)

θ = volumetric water content (cm^3/cm^3)

θ_b = volumetric fraction of constituents (cm^3/cm^3)

θ_e = volumetric fraction of constituents (cm^3/cm^3)

θ_{max} = maximum water content for corresponding node (cm^3/cm^3)

θ_r = minimum water content for corresponding node (cm^3/cm^3)

θ_R = residual water content for node (cm^3/cm^3)

v = fluid flow through porous media (m/s)

χ = general physical quantity

ψ = pressure head ($P/\rho_w \cdot g$)

z = depth below substrate surface (m)

Z = snow or soil layer (m)